Thalamocortical Connectivity
New Insights in Epilepsy Treatment

Byungin LEE, MD

Prof & Director of Epilepsy Center

Inje University, Haeundae Paik Hospital

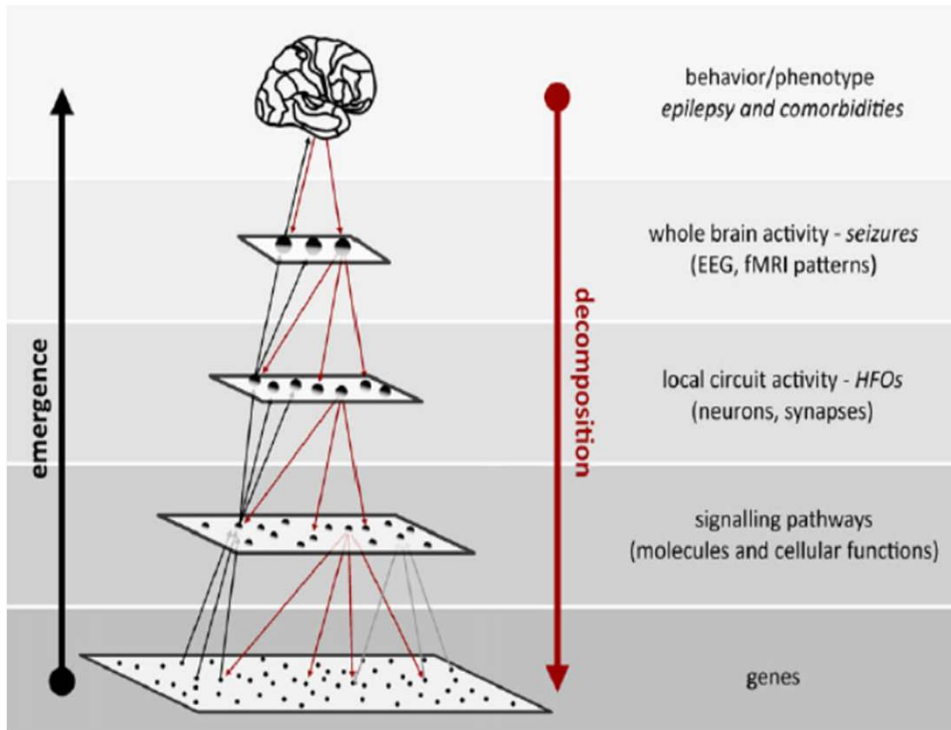**Busan, KOREA**

- **Conflict of Interests: NONE**

Thalamocortical Connectivity:
New Insights in Epilepsy Treatment

- **Epilepsy : A Network Disease**

- **Thalamocortical Networks**
  - *Anatomy*
  - *Structural and Functional Connectivity*
  - *Clinical Studies*

- **Recent Progress and Future Perspectives**

I. Epilepsy: A Network Disease?

➢ Brain is a complex multilevel Network System

A complex system: *any system featuring large numbers of interacting components whose aggregate activity is nonlinear*

RC. Scott et al. Epilepsia. 2018;59:1475–1483
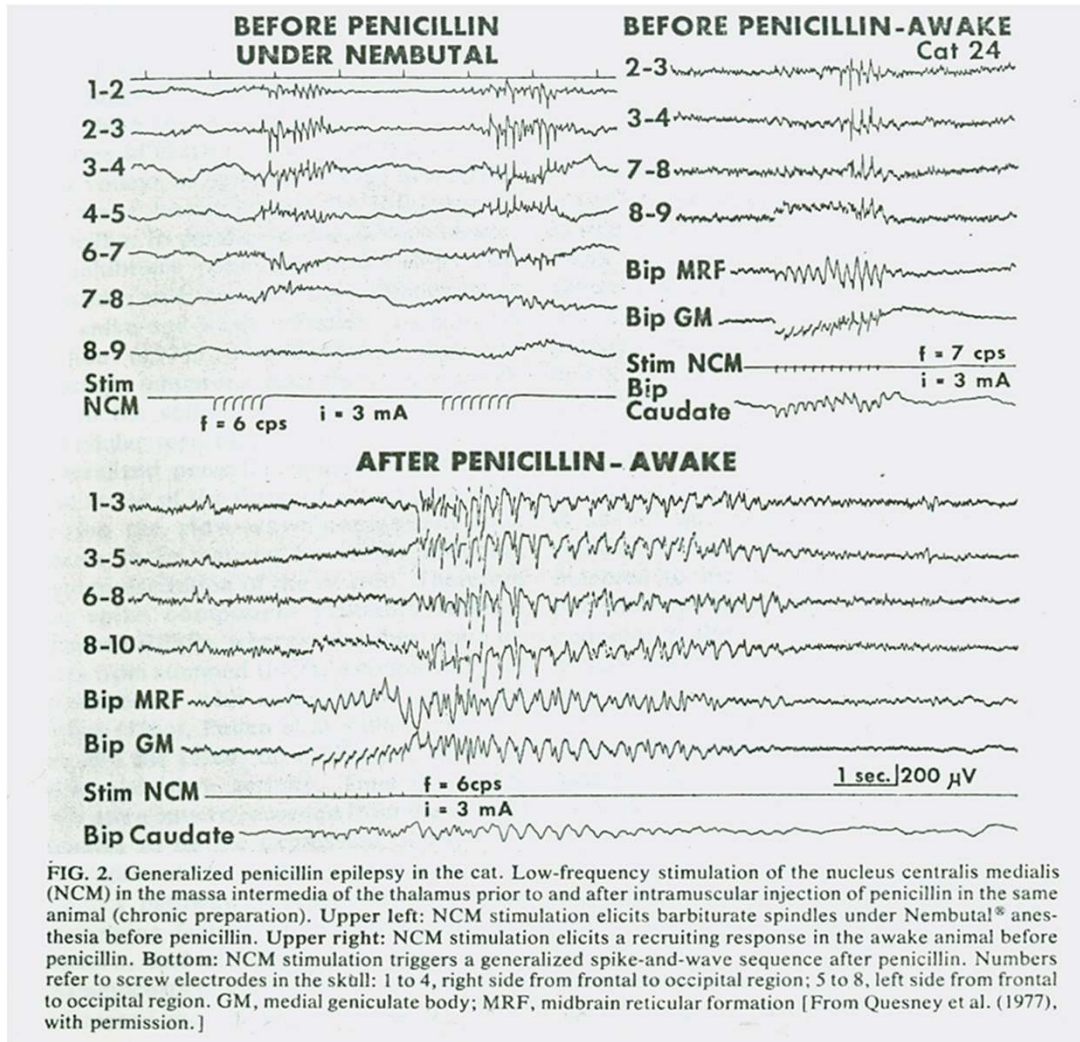
➢ What is Epilepsy Network?

There is no standard framework yet, which is applicable to the pathogenesis of seizures

A. Generalized Epilepsy

Absence Seizures: Model of Feline Generalized Penicillin Epilepsy (FGPE)

FIG. 2. Generalized penicillin epilepsy in the cat. Low-frequency stimulation of the nucleus centralis medialis (NCM) in the massa intermedia of the thalamus prior to and after intramuscular injection of penicillin in the same animal (chronic preparation). Upper left: NCM stimulation elicits barbiturate spindles under Nembutal® anesthesia before penicillin. Upper right: NCM stimulation elicits a recruiting response in the awake animal before penicillin. Bottom: NCM stimulation triggers a generalized spike-and-wave sequence after penicillin. Numbers refer to screw electrodes in the skull: 1 to 4, right side from frontal to occipital region; 5 to 8, left side from frontal to occipital region. GM, medial geniculate body; MRF, midbrain reticular formation [From Quesney et al. (1977), with permission.]

Experiments carried out in the FGPE model demonstrated that:

(1) ↓ thalamic activity by local microinjection of KCl abolishes both spindles and SW discharges;

(2) reduction of cortical excitability by spreading depression makes SW discharges being replaced by spindles in both thalamus and neocortex

→ **Cortex and Thalamus act as a unit: Corticothalamic network**

.

Thalamocortical Networks in Absence Epilepsy

- Which one is the trigger? Cortex vs Thalamus
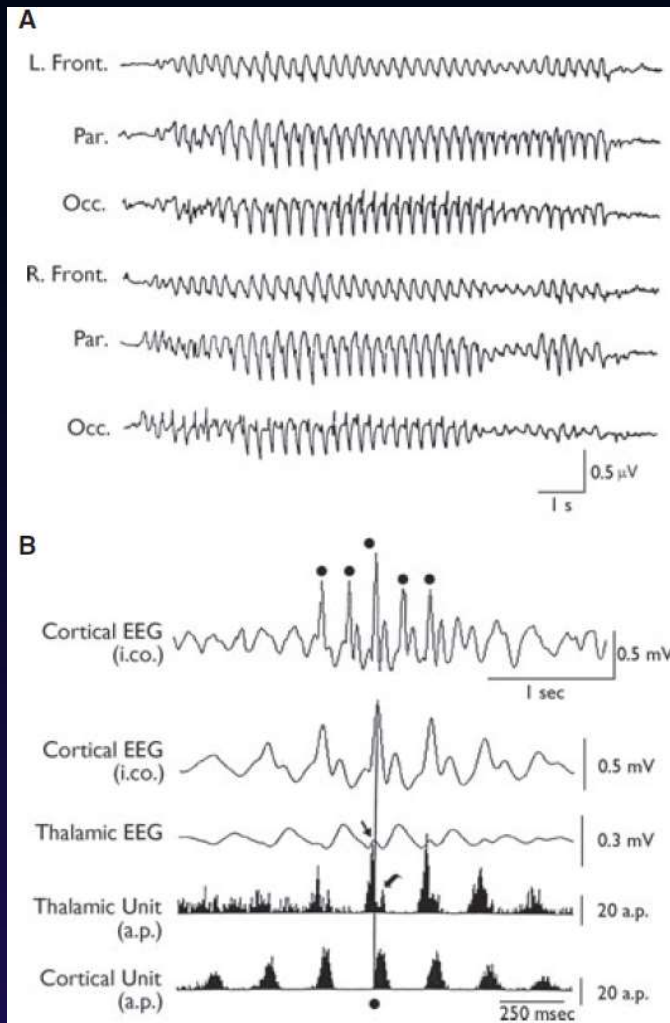
(A) Generalized SW discharges recorded in a cat following intramuscular injection of penicillin.

(B) EEG averages and single-unit peri-event histograms triggered by the negative peaks of the spikes of SW discharges induced by penicillin injection and recorded intracortically (dots in the upper trace). The cortical unit was recorded in the middle suprasylvian gyrus, whereas the thalamic unit was recorded simultaneously from the nucleus lateralis posterior/pulvinar complex. Note the late involvement of the thalamic unit in SW firing as well as the two peaks of firing probability, one (straight arrow) preceding, and the other (curved arrow) coinciding, with the cortical peak of firing probability. The thalamic unit recorded in this experiment was orthodromically activated by electrical stimuli delivered in the cortex middle suprasylvian gyrus (not illustrated)

M.Avoli, Epilepsia 2012;53:779-789

Pathophysiology of Generalized Epilepsy
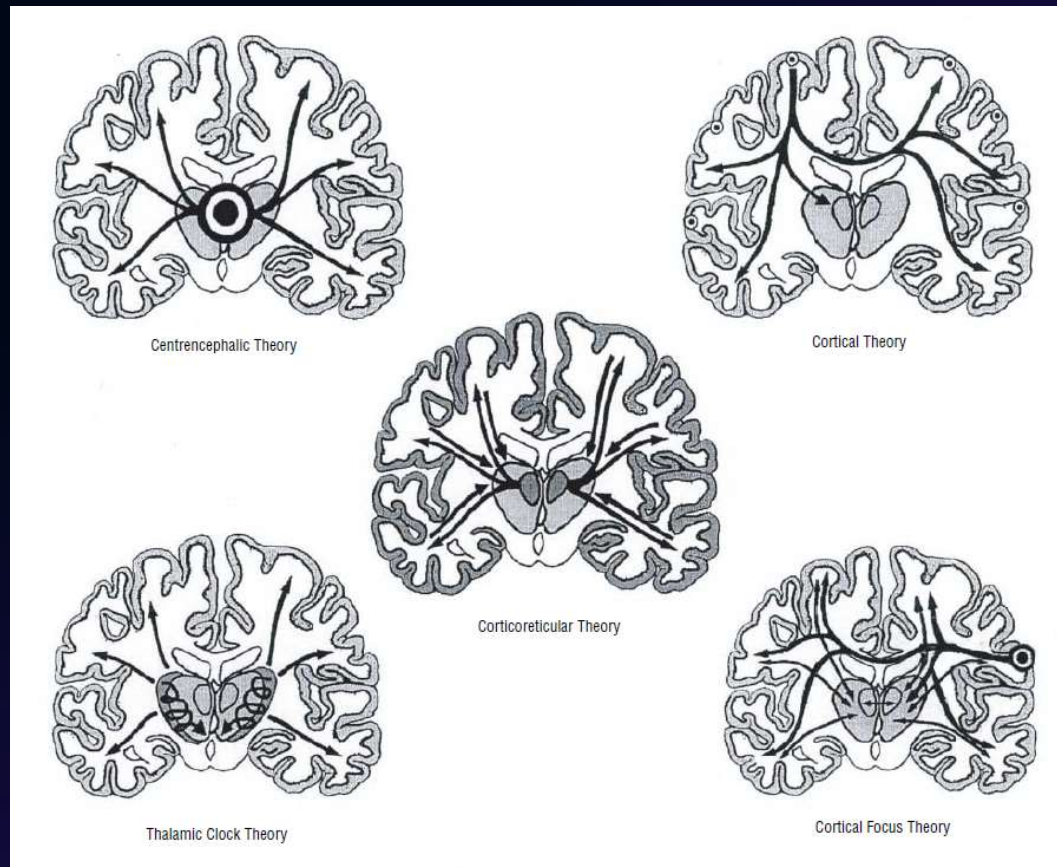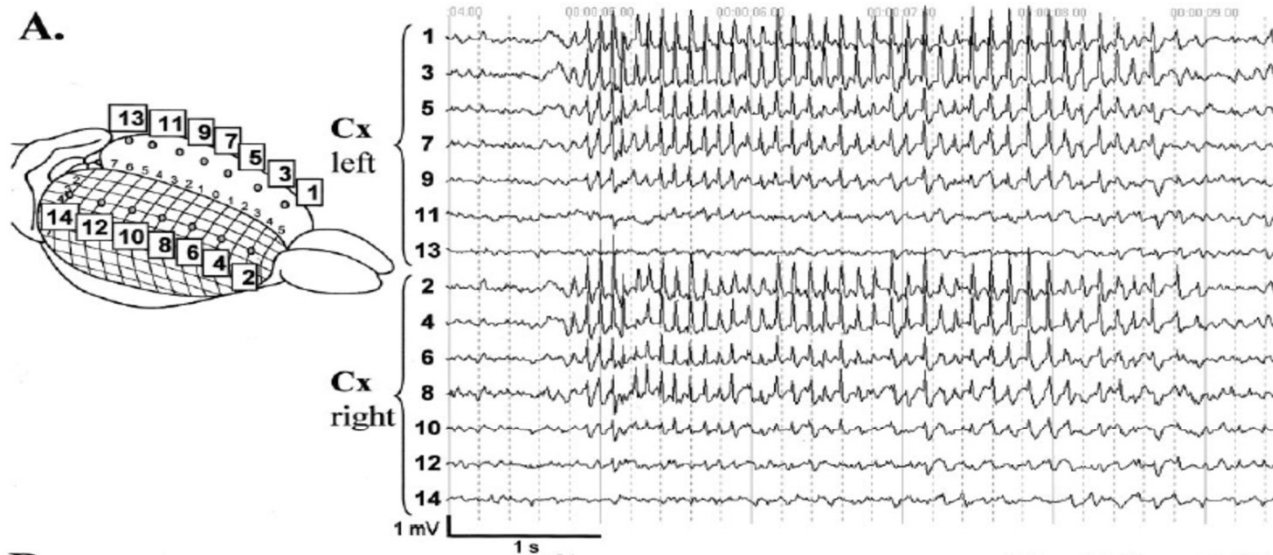## Proposed Theory in Absence Epilepsy

Figure. Schematic impression of the 5 theories on the origin of generalized absence epilepsy.
(Left) **Thalamic theories**: the centrencephalic theory of Penfiled and Jasper and the thalamic clock theory of Buzaki.
(Right) **Cortical theories**: the cortical theory of Bancaud, Luders et al, and Nidermeyer and the cortical focus theory of Meeren et al.
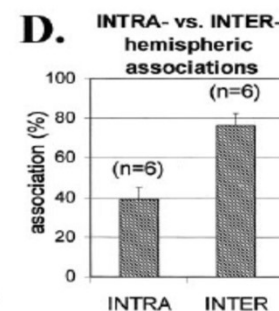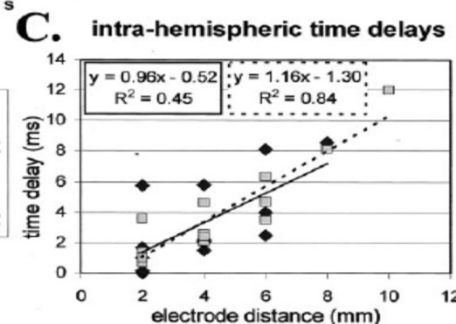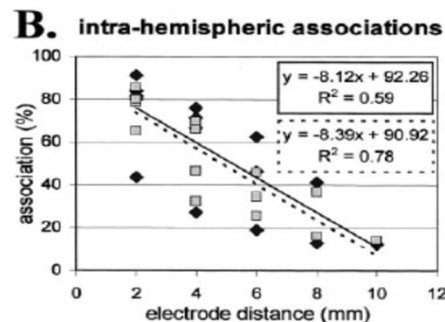(Middle) **Corticoreticular theory** of Gloor
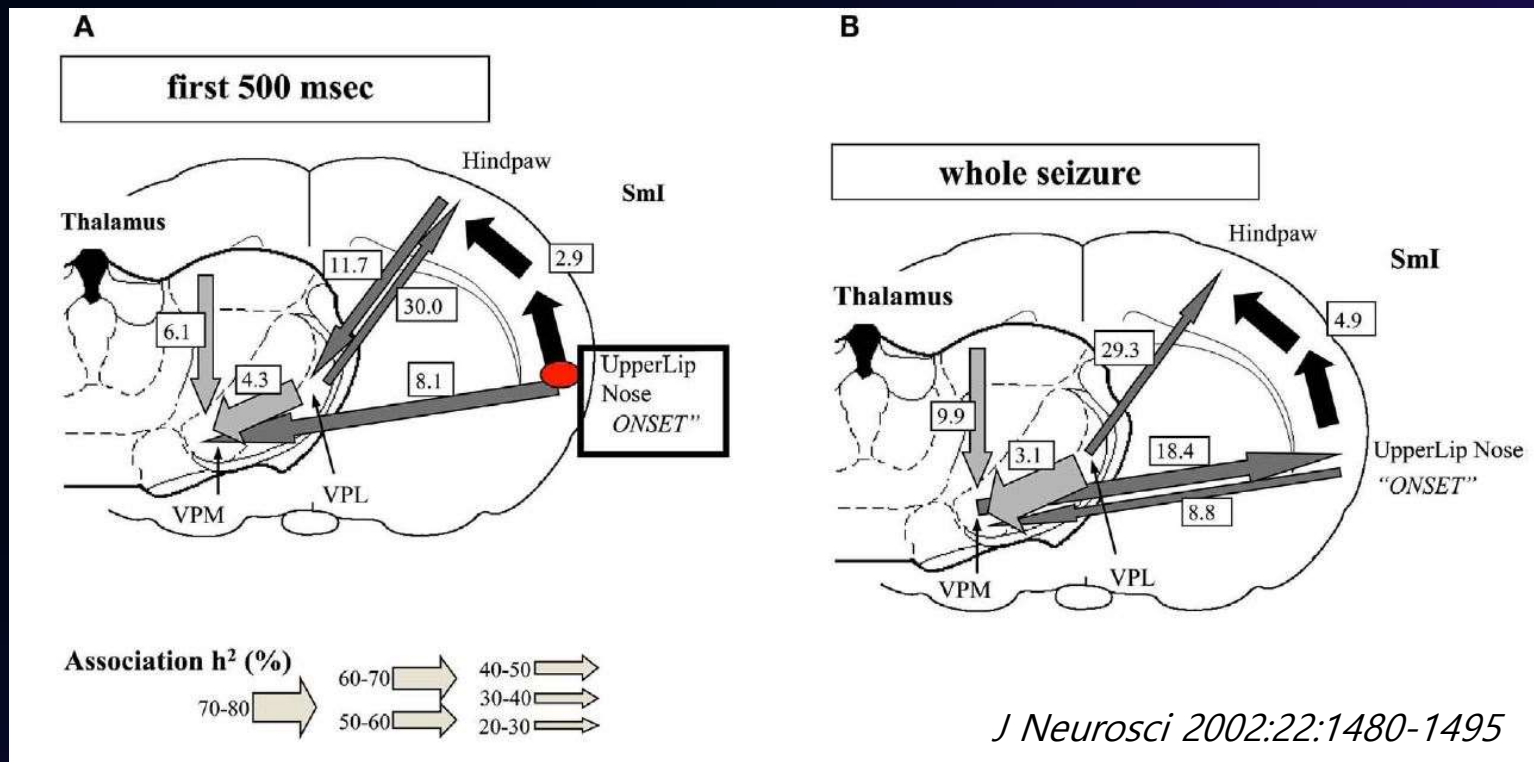
- Does "generalized" spike-wave activity homogeneously involve the entire brain? or are there crucial nodes that are more important than others for the generation of generalized seizures?
- Recording of multisite cortical and thalamic field potentials in WAG/Rij rat revealed a consistent cortical "focus" within the peri-oral region of the somatosensory cortex. The SWDs recorded at other cortical sites consistently lagged this focal site, with time delays that increased with electrode distance

Meeren et al.,
J. Neurosci., 2002, 22(4): 1480–1495

A

first 500 msec

Hindpaw
SmI
Thalamus
11.7
2.9
30.0
6.1
4.3
8.1
UpperLip
Nose
ONSET"
VPM
VPL

Association h² (%)
70-80
60-70   40-50
50-60   30-40
        20-30

B

whole seizure

Hindpaw
SmI
Thalamus
29.3
4.9
9.9
3.1   18.4
UpperLip Nose
"ONSET"
8.8
VPM   VPL

J Neurosci 2002:22:1480-1495

Evolution of absence seizures in the rat genetic model: (A) corticocortical (represented by the black arrows), intra-thalamic (light gray arrows), and cortico-thalamic (dark gray arrows) interdependencies during spontaneous absence seizures in the WAG/Rij rat as established by the non-linear association $h2$ analysis. The thickness of the arrow represents the average strength of the association, and the direction of the arrowhead points to the direction of the lagging site. The values represent the corresponding average time delays in milliseconds. This example represents the average of 10 seizures of one rat. The relationships are stable for the first 500ms of the absence seizure. A consistent cortical onset was found in the upper lip and nose area of the somatosensory cortex (SmI), because this site consistently led the other cortical recording sites. The hindpaw cortical area was found to lag by 2.9ms on average with respect to this focal site. Within the thalamus, the laterodorsal (LD) nucleus was found to consistently lead other thalamic sites. The ventroposterior medial (VPM) nucleus was found to lag behind the ventroposterior lateral (VPL) nucleus, with an average time delay of 4.3 ms. Concerning cortico-thalamic interrelationships, the cortical focus site consistently led the thalamus (VPM), with an average time delay of 8.1 ms.
(B) The relationships found when the whole seizure is analyzed as one epoch.
The same cortical focus as during the first 500ms was found consistently. Compared with the first 500 ms, the time delay from the cortical focus with respect to the non-focal cortical sites increased. Furthermore, the strength of association between VPL and VPM also increased. The direction of the cortico-thalamic couplings changed. For the non-focal cortical sites, the thalamus was found to lead during all seizures. For the focal cortical site, the cortex was found to lead during two seizures, whereas the thalamus was found to lead during seven seizures

- The histogram shows the ratio of sodium channel mRNA levels in the neocortex of 6-month-old WAG/Rij (epileptic) rats compared to age-matched Wistar (non-epileptic control) rats. At anatomical location "E," corresponding to barrel somatosensory cortex, there is a statistically significant increase in **Nav1.1 (white bars)** and **Nav1.6 mRNA (black bars),** but not Nav1.2 mRNA (gray bars), in the epileptic animals compared to control animals. Anatomical locations of tissue plugs used for quantitative PCR analysis are indicated on inset drawing of rat brain.. Data are plotted as mean ± SE; n = 8 animals, ∗p < 0.05, ANOVA with post hoc Fisher's least significant difference analysis with Bonferroni adjustment.
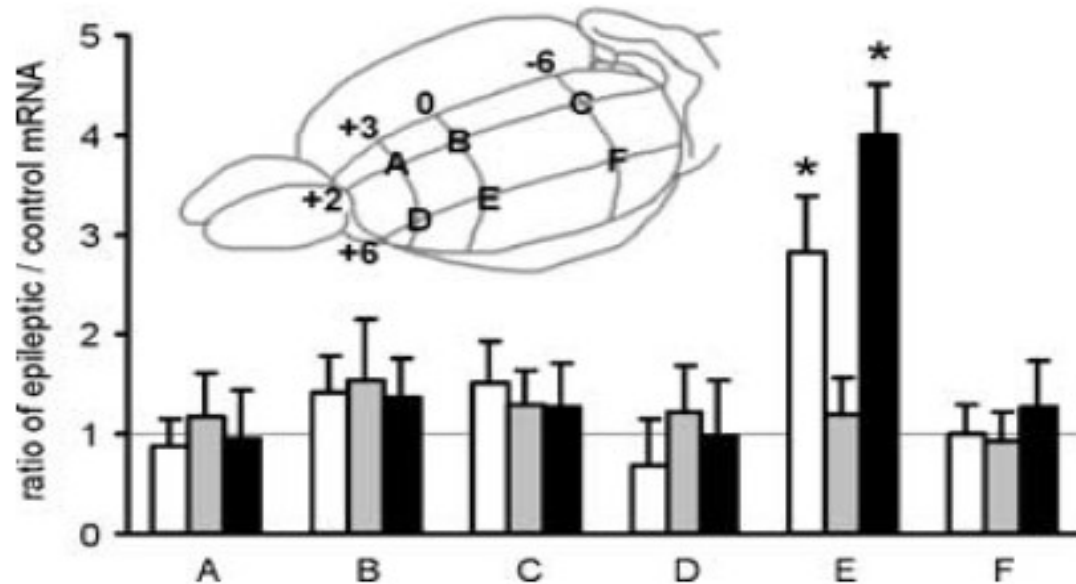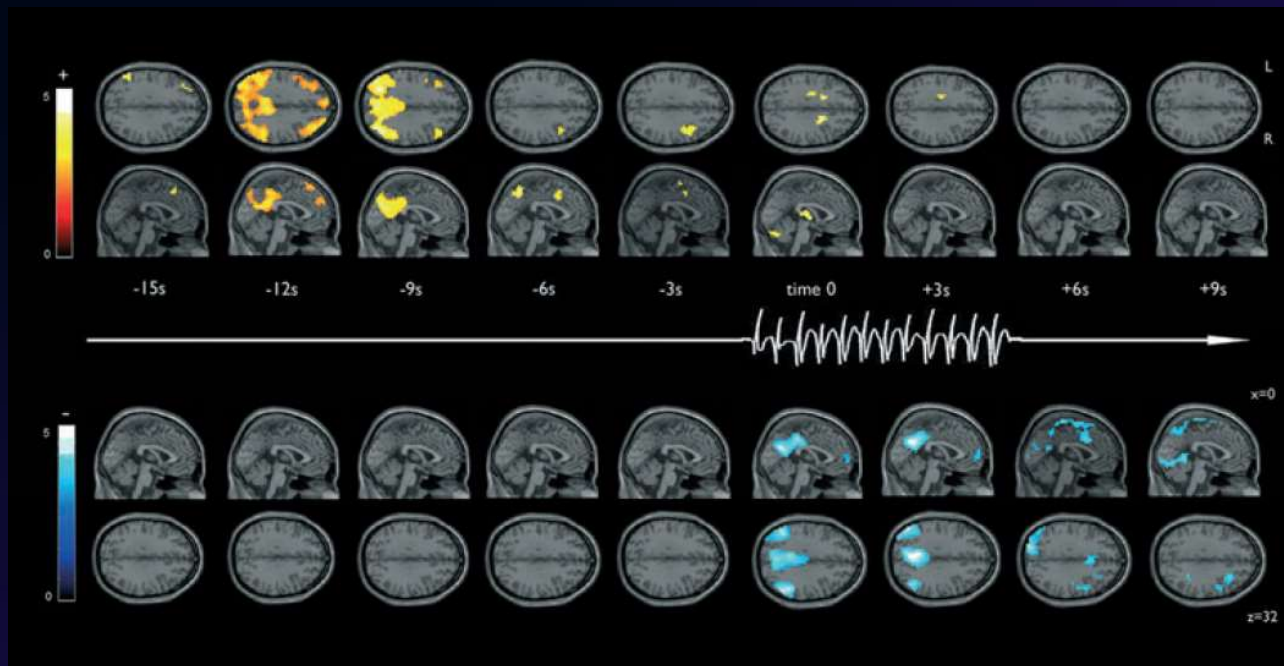
What triggers 3Hz SWC? Cortex vs Thalamus

- *Benuzzi et al.* (Epilepsia 2012;53:622-630)

 n = 15pts with IGE underwent EEG-fMRI co-registration

BOLD changes preceding and following GSWDs. The dynamic analysis (second-level random-effect group analysis) of the 15 patients is reported. Axial and sagittal sections (MNI coordinates) displaying BOLD fMRI changes (p < 0.001) are shown for each time window (serious of successive HRF models at 3 s intervals from -15 to +9 s). Increases in BOLD signal (Red) are observed before GSWDs in posterior and anterior cortical areas, and then at GSWD onset thalamic involvement is evident. Decreases in BOLD signal (blue) are observed from the onset of GSWD until several seconds after it, approximately in the same cortical areas. The white arrow is a representation of the EEG activity, flat to symbolize rest, and spike-and-wave of 4 s long, as the mean duration of GSWDs cross patients.

- **H. Blumenfeld** [Epilepsia, 2003; 44(Suppl. 2):7–15]

➤ Enhanced "Burst Firing of Action Potentials" in one region of the nervous system, such as the cortex, transform the entire thalamocortical network from normal activity to spike-and-wave seizures

  - Brief burst of corticothalamic neurons → $GABA_A$ receptor in the thalamus
    → Spindles

  - ↑ burst firing in corticothalamic neurons → ↑$GABA_B$ receptor in the thalamus
   → slower, synchronous oscillations of SWC
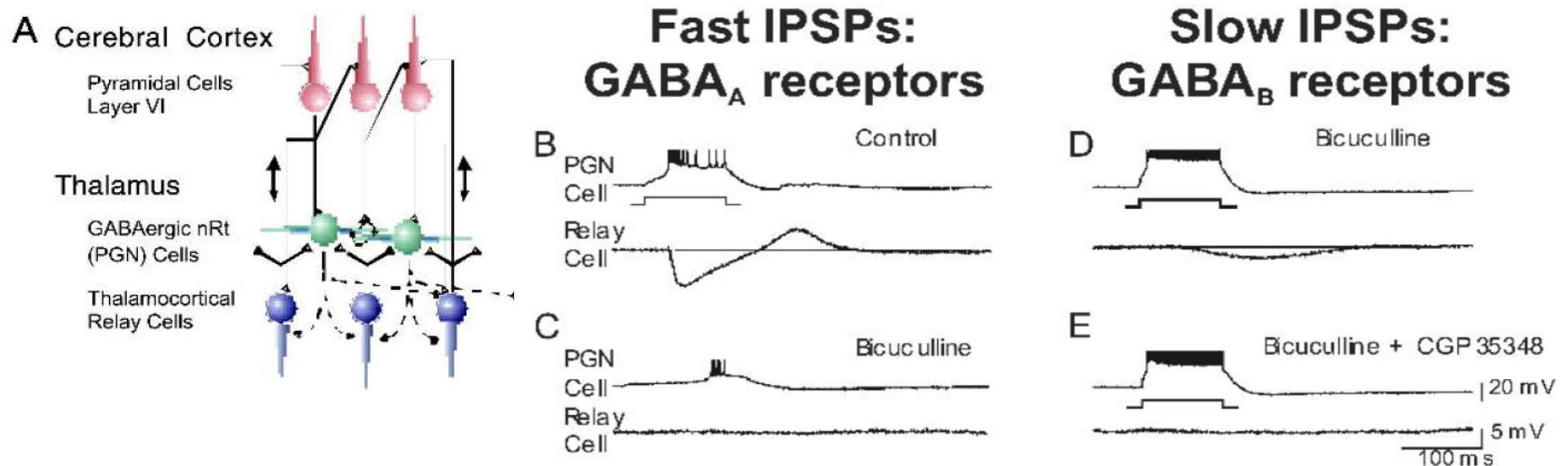
Bicuculiline: GABA $_A$ receptor antagonist
CGP 35348: GABA $_B$ receptor antagonist

B. Focal Epilepsy

● Focal SZ: originating within networks limited to one hemisphere. For each Sz type, ictal onset is consistent from one Sz to another with preferential propagation patterns that can involve the contralateral hemisphere (ILAE 2010).

● S Spenser (Epilepsia 2002;43:219-227) :

▪ *Functionally and anatomically connected sets of cortical and subcortical structures in which activity in any part affects activity in all the others*

▪ The entire Epilepsy Network participates to the expression of the seizure activity

→ **any part of EN** can be entrained to the initial electrical events at "seizure onset"

→ Location of Seizure Onset as well as Ictal EEG onset patterns may vary according to the initiating part of EN

→ However, clinical seizures are stereotyped, because the network as a whole is responsible for the manifestations of the seizures

(minor variation may reflect propagation of seizure activity)

Seizure #1 in a patient with epilepsy in the Medial Temporal/Limbid Network
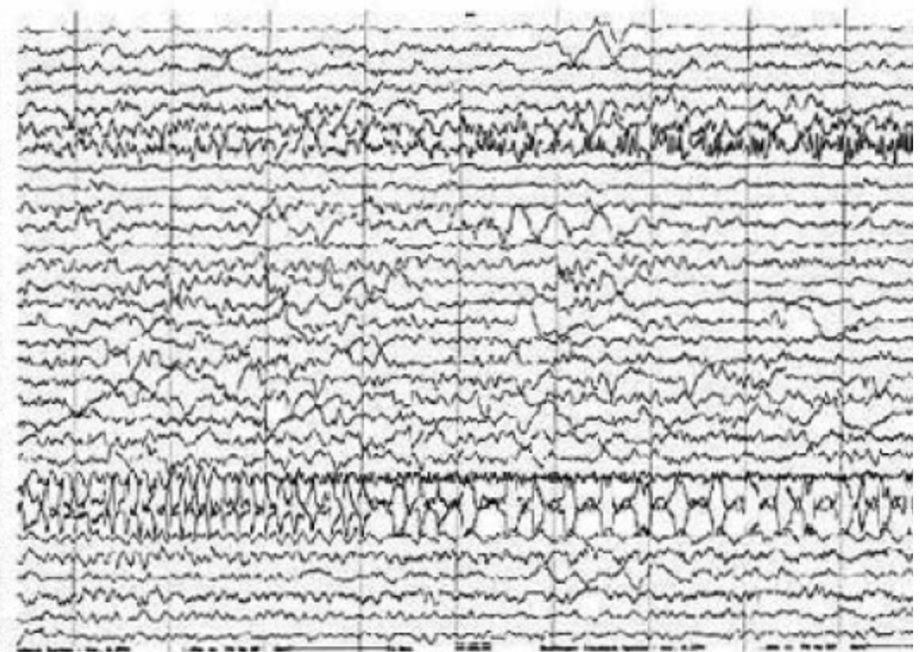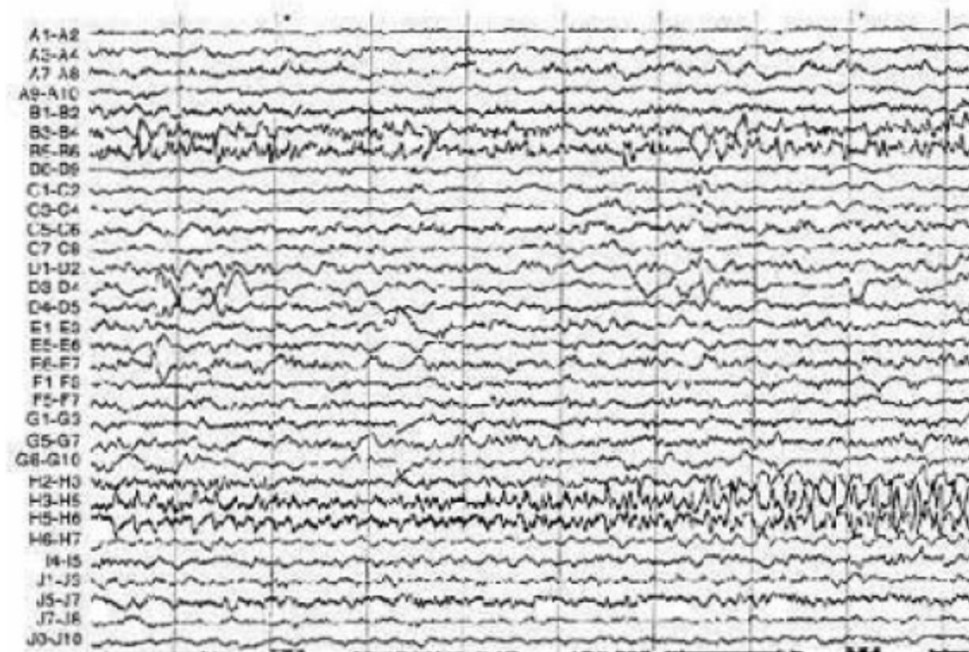
Seizure #2 from same patient of Figure 1.
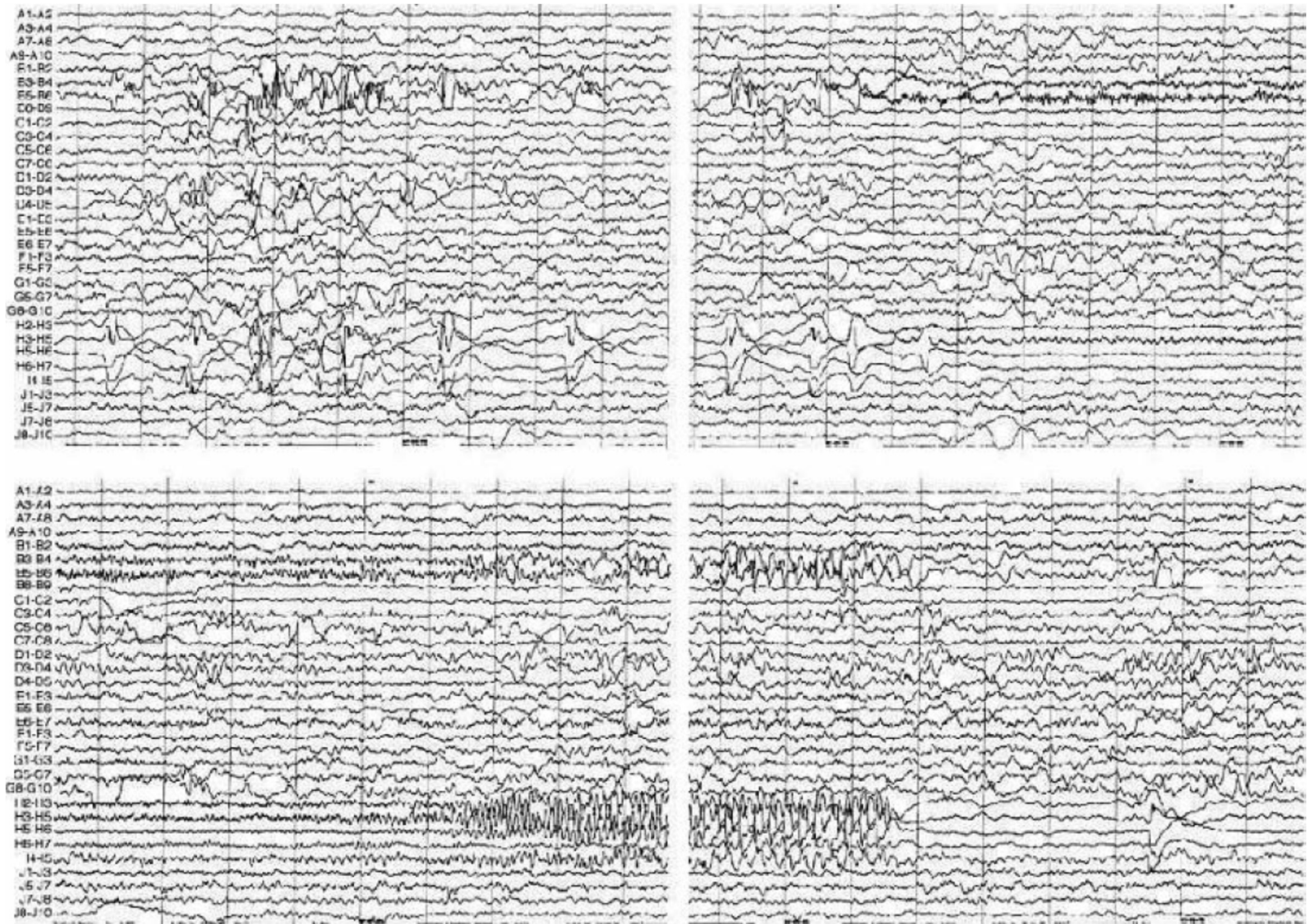
B. Focal Epilepsy

● **Thalamus a primary component of Epilepsy Network?**

▪ **EH Bertram, et al,** (Epilepsia, 2008; 49:256–268)

- Simultaneous recording from Hippocampus, Amygdala, and mesial dorsal nucleus of thalamus in Rats, after direct infusion of the GABA antagonist bicuculline or agonist muscimol to the MDN

- **Results:** Drugs enhancing excitatory drive or blocking GABA → ↑ prolongation of SZ

  Drugs enhancing GABA activity→ ↓SZ duration

  Infusion of the compounds lateral to the MDN → No affect on seizure duration.

- **MDN** has a significant role in the primary seizure circuits of limbic seizures as well as in spread of seizure activity to other regions.
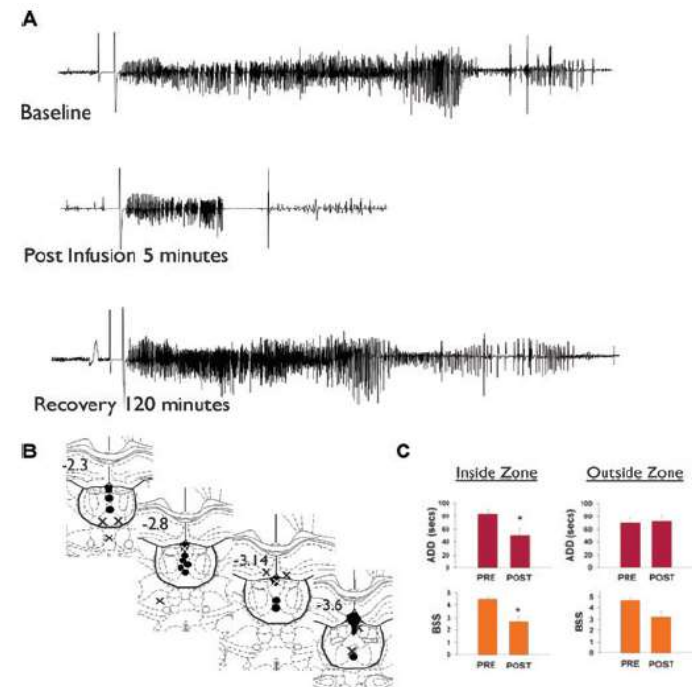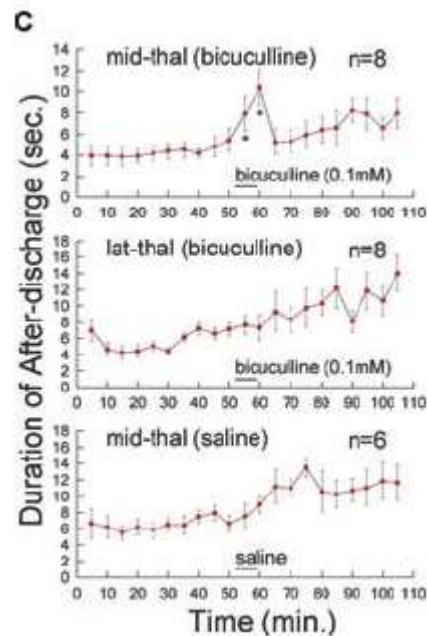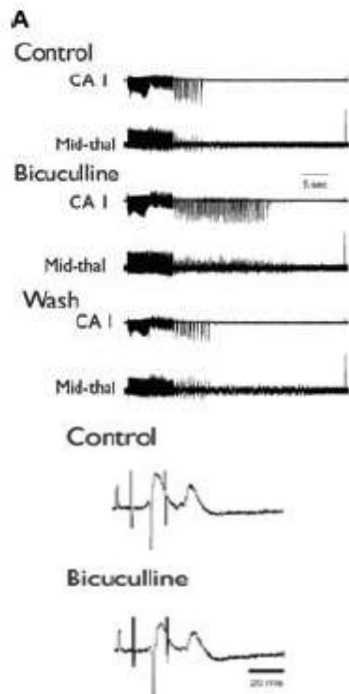
- **Paz et al.** (*Nature Neurosci 2013:16:64-70):* "Closed-loop Optogenetic Control" of thalamus in Post-stroke Epilepsy model in Rats

- *Focal cortical infarction* → alter the intrinsic excitability of interconnected thalamic neurons as hyperexcitable to form hyperexcitable *Thalamocortical Network*
  → spontaneous epileptiform discharges involving both cortex and thalamus
  → selective optical inhibition of thalamocortical neurons interrupts ongoing epileptic seizures.
  (the spatial distribution of hyperexcitable thalamic neurons were quite restricted to the directly interconnected area to the infarction)
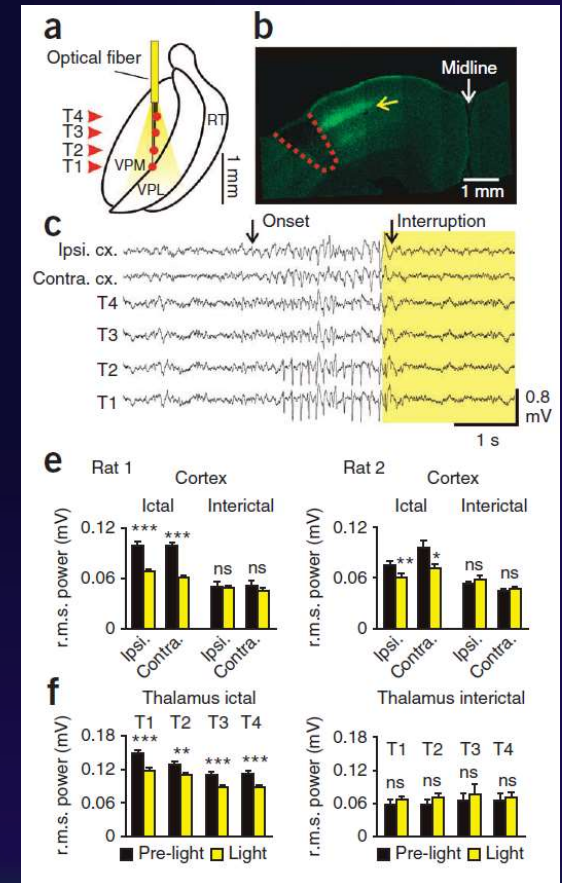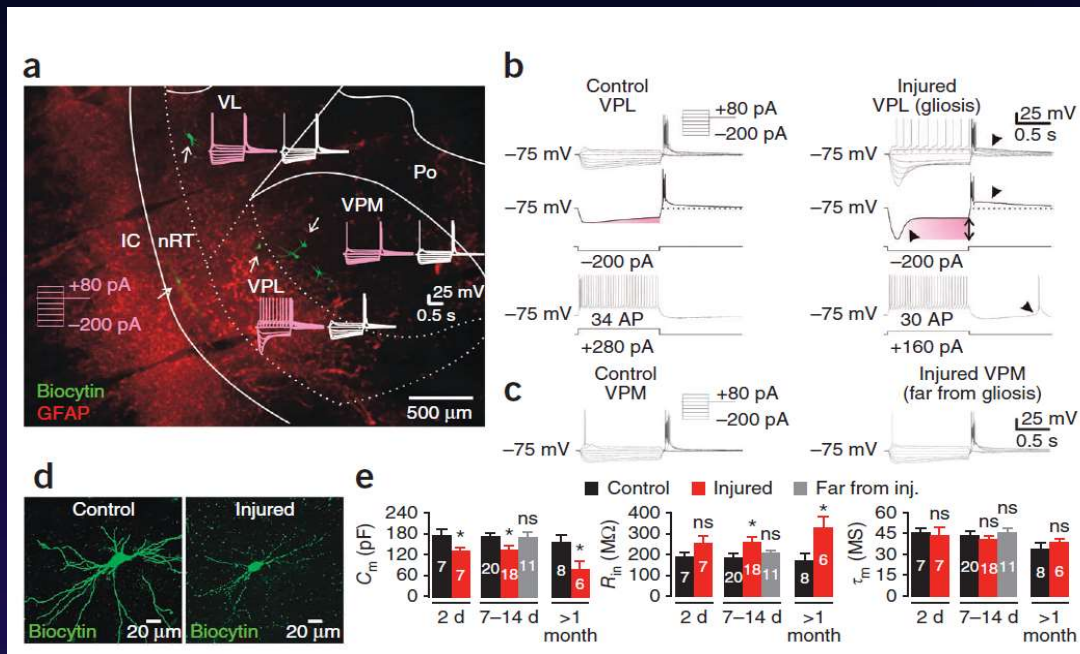
Functional Anatomy of Seizure Network
(EH Bertram, Exp Neurol 2013)
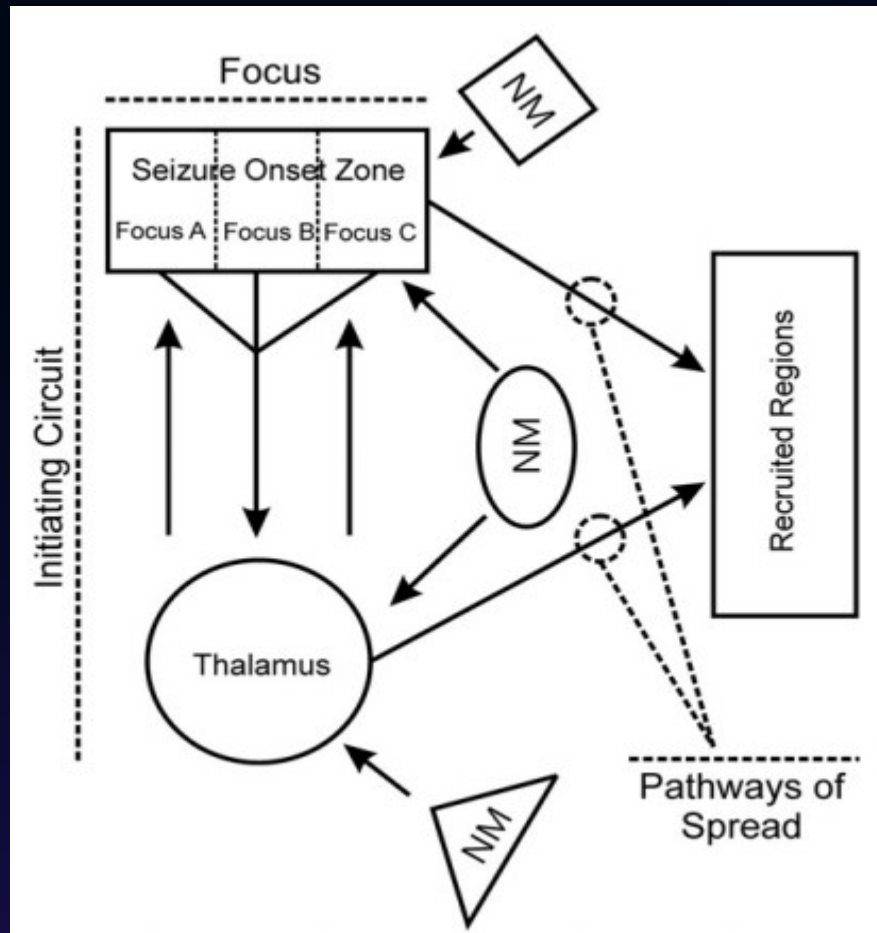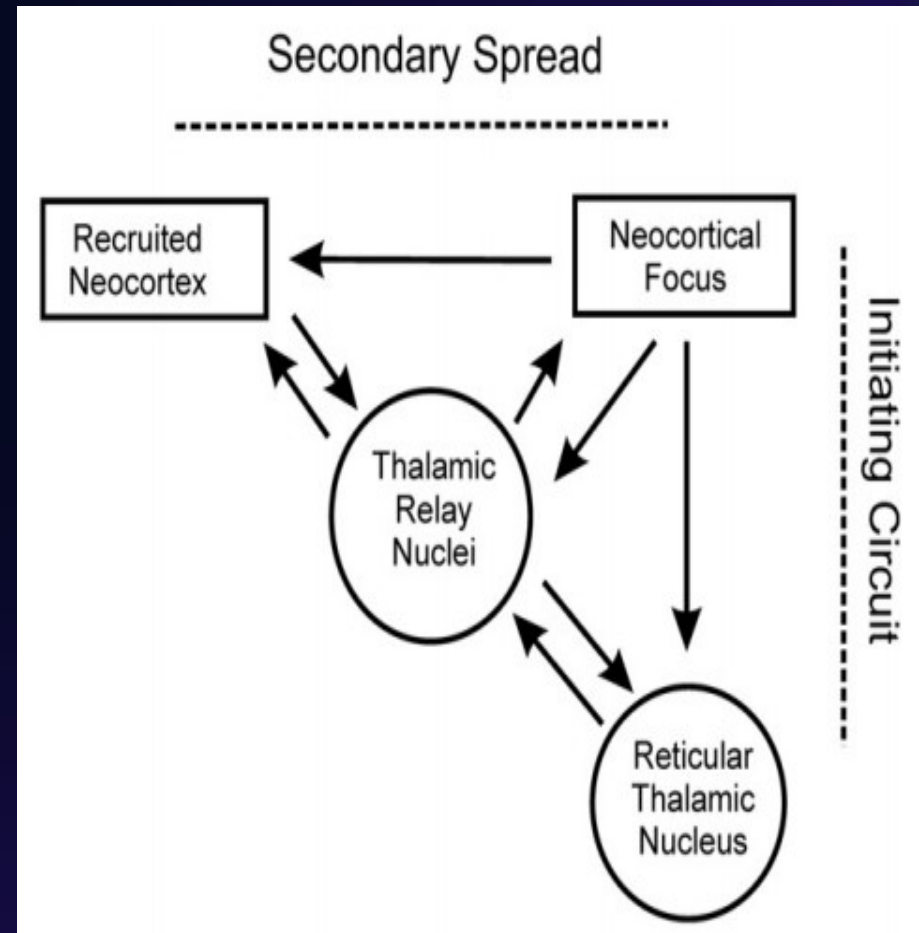
Focal Seizures   **Generalized Seizure**

SUMMARY

● Thalamus is a key structure in the Epilepsy Network of both Generalized and Focal Epilepsy,

● The identification and differentiation of "Primary Epilepsy Network" in clinical epileptology is uncertain yet, which is the Major Research Target

1. Anatomy

- Thalamus is a relay station in the center of brain conveying nearly all modalities of inputs to the cortex, e.g., sensory inputs, motor inputs from cerebellum and BG, limbic inputs, widespread modulatory inputs involved in arousal and sleep-wake cycles, etc.

- Some thalamic N have specific topographical projections to cortical areas, while others project more diffusely. They typically receive reciprocal feedback connections from cortical areas of their projection

- Thalamus is divided into a **Medial, Lateral, and Anterior Nuclear Groups** by a Y-shaped white matter, called the internal medullary lamina. Nuclei located in the internal medullary lamina itself are called the **Intralaminar Nuclei**

- **Midline thalamic Nuclei** are thin collection of nuclei lying adjacent to the third ventricle

- **Thalamic reticular Nuclei,** extensive but thin sheet enveloping lateral aspect of thalamus

- **Pulvinar:** N occupying most of posterior thalamus, projecting widely to parietal, temporal, and occipital association cortex

- **Lateral Geniculate N:** Visual relay N
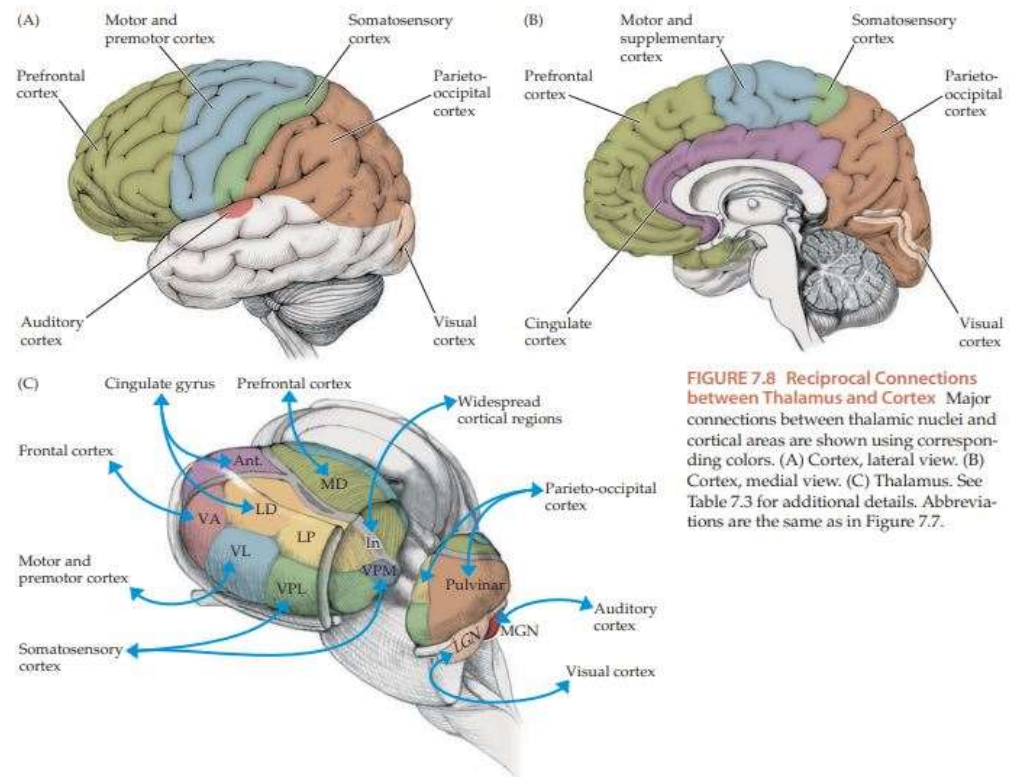
- **Medial Geniculate N:** Auditory relay N

FIGURE 7.8 **Reciprocal Connections between Thalamus and Cortex** Major connections between thalamic nuclei and cortical areas are shown using corresponding colors. (A) Cortex, lateral view. (B) Cortex, medial view. (C) Thalamus. See Table 7.3 for additional details. Abbreviations are the same as in Figure 7.7.

❖ **KS Rockland** (Eur J Neurosci, 2019; 49:969–977)

● Single axon analysis revealed two broad classes of corticothalamic (CT) Neurons

▪ CT neurons in *layer 5 (class II) have spatially compact thalamic fields, but highly spatially divergent cortical collaterals.*

▪ *CT neurons in layer 6 (class I) have highly divergent thalamic fields, but delimited, low divergent cortical collaterals.*

● Reciprocating thalamocortical (TC) axons have multiple clustered and divergent arbors, making synapse across the whole cortical layers

● Significance of these morphological relationships? Anatomical connectivity-defined parcellations of the thalamus using anterograde tracing do not cleanly map onto histologically defined thalamic nuclei, instead encompassing multiple nuclei and even multiple nuclear groups (Hunnicutt et al. 2014)

● How to identify specific CT networks?
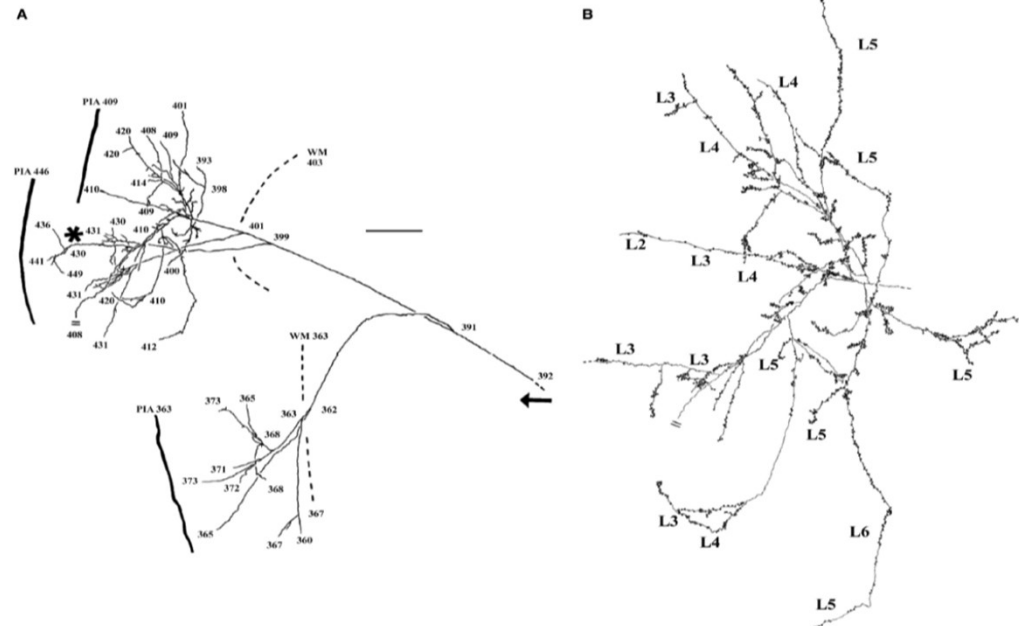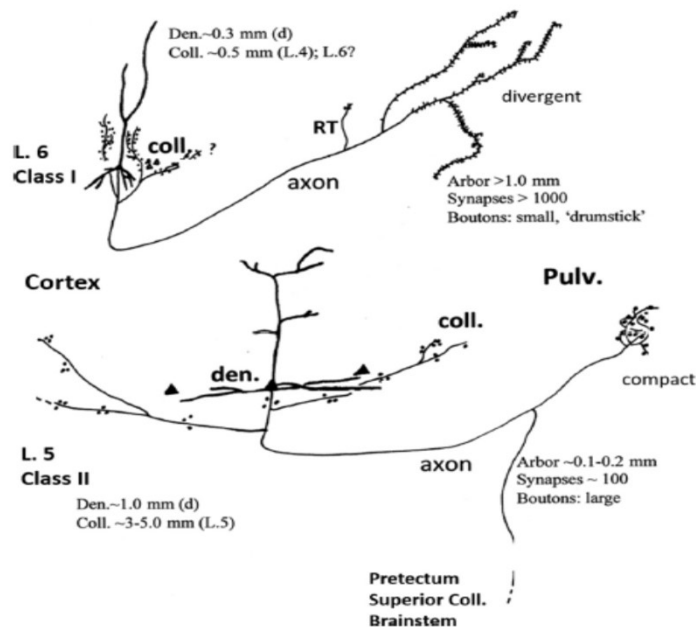
- **J O'Muircheartaigh et al.** (Cerebral Cortex, 2015;25: 4477–4489)
- Noninvasive mapping of structural and functional connectivity of the human thalamus using diffusion-weighted and resting-state functional MRI (N=102 adults)
- Tensor ICA of the probabilistic diffusion tractography data resulted in 25 and 26 spatial components for the left and right thalamus, → The output was back-reconstructed onto the thalamus, revealing the specific thalamic origins for these presumed white matter bundles
- Using resting-state fMRI in the same subjects, whole-brain functional connectivity with these thalamic seed regions resulted in highly significant anatomically specific functional connectivity in cortical and subcortical regions, which were broadly be reduced to a subset of 7 core-network
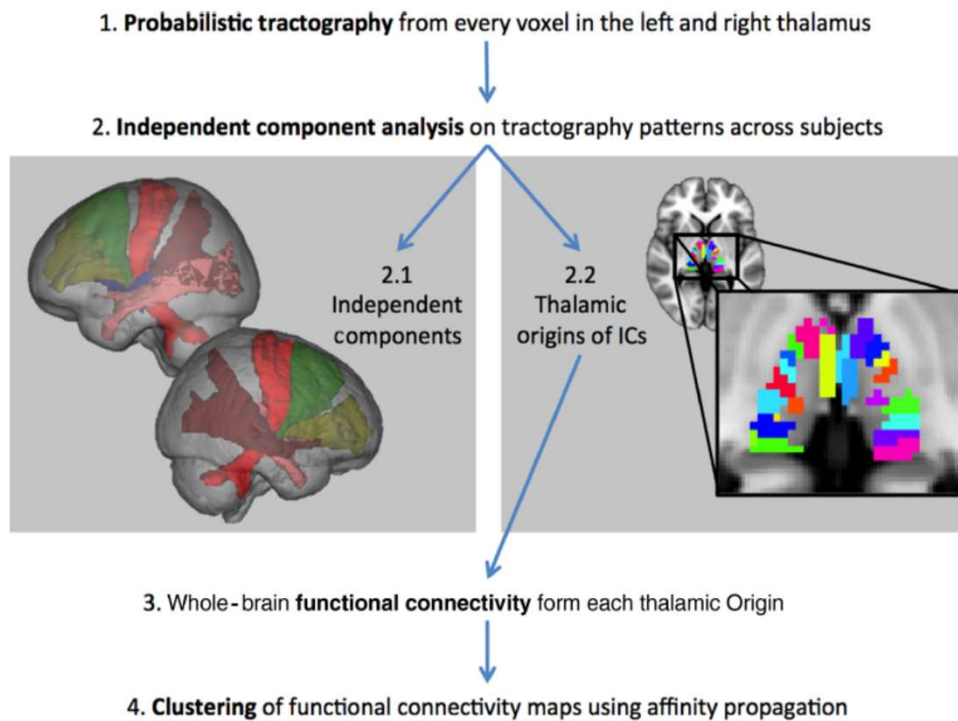

Basic workflow showing the main analysis steps
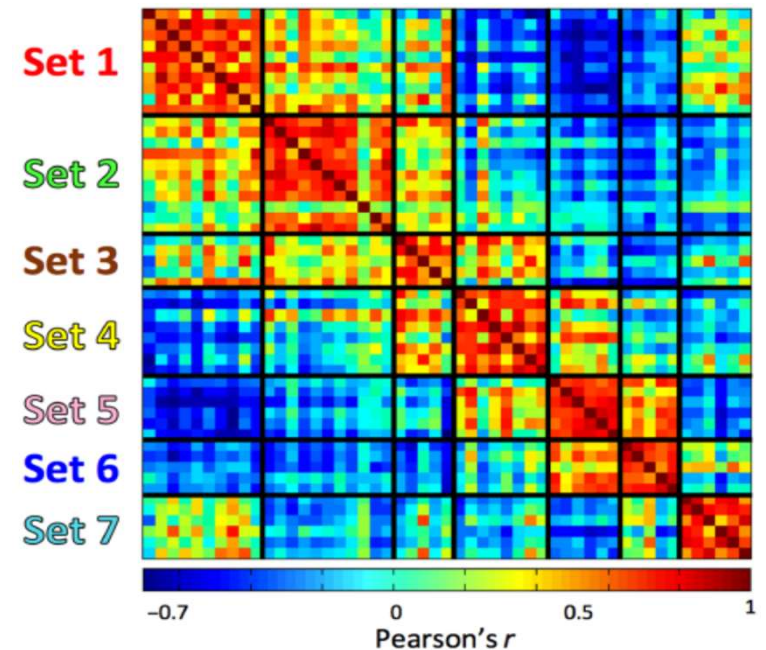
Correlation matrix between spatial connectivity networks for each thalamic region identified using DTI Connectivity

- The underlying thalamic origin of these sets demonstrated a pattern of medial-to-lateral bands, eminating radially from the mesial aspect of each thalamus and The shared regions of connectivity show a distinct rostrocaudal profile across the cortical midline that maps onto the anteromedial-posterolateral structural connectivity profile in the thalamus.
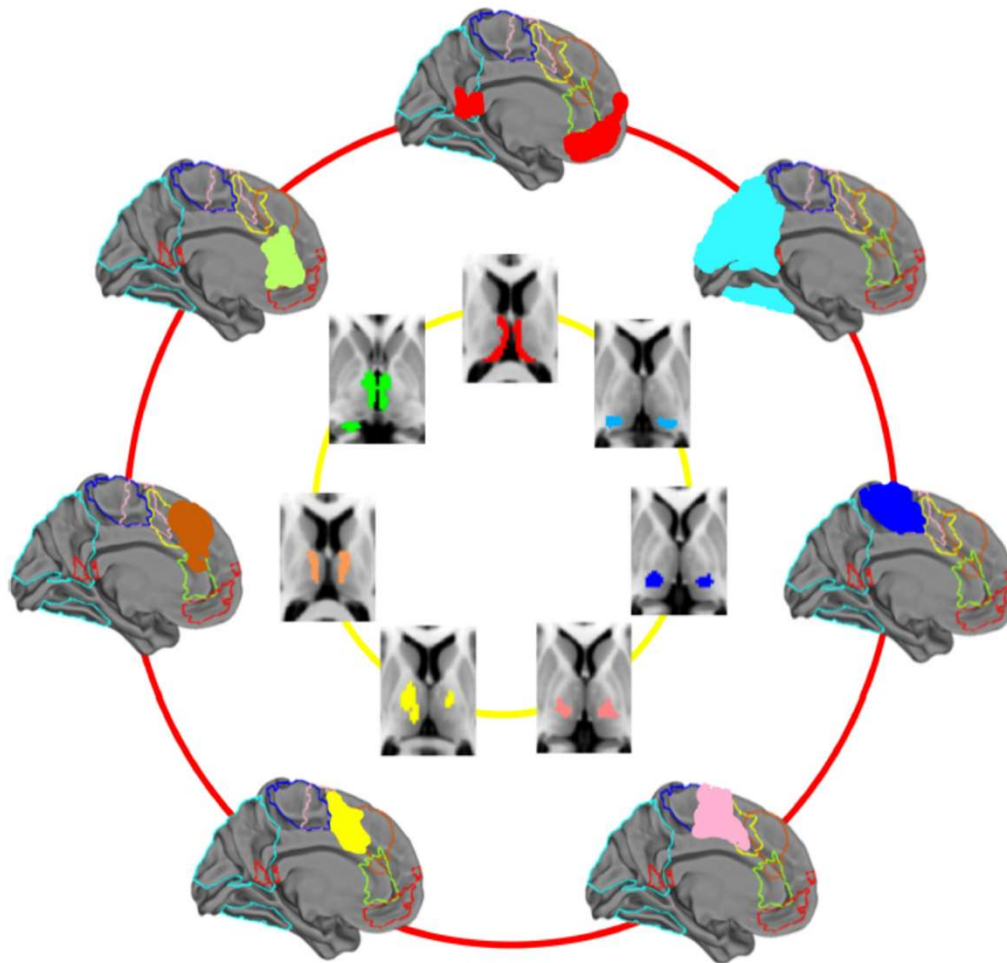
Set 1. medial orbitofrontal cortex, bilateral middle temporal gyrus, bilateral hippocampus, posterior cingulate and retrosplenial cortex

Set 2: ventral anterior cingulate, ventral caudate and anterior putamen

Set 3: Frontoparietal network including middle frontal gyrus, frontal opercula, and supramarginal gyrus

Set 4: bilateral insula, premotor and SMA and supramarginal gyrus

Set 5: Precentral gyrus, SMA, Putamen, and cerebellum

Set 6: Pre and postcentral gyri

Set 7; Parietal and occipital, ventral temporal cortex

fcMRI
- Nodes: BOLD time series
- Edges: Correlation

DTI
- Nodes: Voxels/regions
- Edges: Tract volume, fiber density

Structural MRI
- Nodes: Cortical thickness, subcortical gray matter volume, 3x3x3 voxel cubes
- Edges: Correlation

Surface EEG
- Nodes: Electrode recordings
- Edges: SL, PLI, mean phase coherency

icEEG
- Nodes: Electrode recordings
- Edges: SL, PLI, DTF

MEG
- Nodes: MEG channel recordings
- Edges: PLI, cross-correlation, mean phase coherency

Cell cultures
- Nodes: Electrode spike timing recordings
- Edges: Cross-covariance

Simulated neuron models
- Nodes: Neurons
- Edges: Number of synaptic connections

(a)

(b) Create adjacency matrix

(c) Functional graph

(d) Clustering coefficient

(e) Path length

(f) Hubs and modules

Overview of graph theory analysis.
Nodes and edges for the brain graph are first defined specific to each modality(a) an adjacency matrix is constructed based on any of a variety of association measures (b). Values of the adjacency matrix are used to construct a graph of the brain network (c). Various graph theory metrics can then be calculated (d–f). In (d), The clustering coefficient of the red node can be calculated as the ratio of the number of existing connections between these direct neighbors (two) to the number of possible connections between these direct neighbors (six), or 1/3. In (e), the characteristic path length between the red and blue nodes is the least number of edges between them (two). In (f), there are two sets of interconnected neurons which form so-called ''modules,'' and are interconnected though the green ''hub'' through which most of the shortest path lengths pass in this network. SL = synchronization likelihood, PLI = phase lag index, DTF = directed transfer function   **Z. Haneef, S. Chiang / Seizure 23 (2014) 809–818**

Graph theory: A mathematical framework to study complex network topology. Networks are formalized as collections of nodes interconnected by edges

Definition	
Assortative network	Network in which hubs tend to connect to each other. Assortativity is most commonly measured using the *assortativity coefficient* or *neighbor connectivity*
Assortativity coefficient	Calculated as the Pearson correlation coefficient of degree between pairs of linked nodes. Positive values indicate nodes with similar degree; negative values indicate nodes with dissimilar degree. Measures the propensity of nodes to connect to others with similar degree
Betweenness centrality	Calculated as the number of all geodesics (shortest paths) in a network that pass through a given node, divided by the total number of geodesics in the network. Provides a measure of the node's importance. Nodes with high betweenness centrality are located on highly traveled paths
Characteristic path length	Calculated as the average number of edges along the shortest distances between all possible pair of network nodes. Lower characteristic path length indicates higher level of global network integration. Measure of long-distance connectivity, as well as network's ability for serial information transfer
Clique	A subset of nodes such that an edge exists between each pair of nodes in the subset
Closeness centrality	Calculated as the inverse of the sum of the distance of a node i to all other nodes. Measure of how long it takes for information to spread from a given node to others in the network
Clustering coefficient (local)	Calculated as the number of edges between the nodes within the neighborhood of a given node, divided by the total number of possible edges between the nodes in the neighborhood. Measure of how close a given node's neighbors are to forming a clique
Clustering coefficient (network)	Calculated as the mean local clustering coefficient, averaged over all nodes in the network. Measure of the degree to which regions cluster, providing measure of local connectivity
Degree centrality (degree)	Calculated as the number of edges directly linking a node to other nodes in the network. Higher degree centrality indicates regions that are more connected to the rest of the network
Degree distribution	The probability distribution of the degrees in a network
Disassortative network	Network in which hubs tend to avoid connecting to each other (see "assortative network")
Edge weight correlation	Similarity of the weighted connections to one region. High edge weight correlation increases efficiency of information processing, although excessively high edge weight correlations increase epileptogenicity
Eigenvector centrality	The eigenvector centrality of node i is calculated from the ith element of the first eigenvector of the adjacency matrix. Identifies nodes that are connected to highly connected nodes (i.e. nodes that are connected to nodes that are central within the network)
Global efficiency	Calculated as the average of the inverse of the shortest path lengths in a network. Measure of network's ability for parallel information transfer
Indegree	A directed graph measure; calculated as the number of nodes that point to a particular node. Reflects the number of incoming connections to a node
Leverage centrality	Calculated as the ratio of a node's degree relative to the degree of neighboring nodes. Provides a measure of the node's importance, by estimating the extent to which a node's neighbors rely on it for information. Positive leverage centrality indicates that a node is more central to the network than its neighbors and is a "hub," whereas negative leverage centrality indicates that the node is less central than its neighbors
Local efficiency	Calculated as the inverse of the average shortest path connecting the given node with all other nodes. Provides a measure of the efficiency of a given node in communicating with the rest of the brain
Module	A subgraph of nodes which are more strongly connected to each other than the rest of the network. Modules often correspond to different functional aspects of the network
Network hub	Node with degree centrality greater than the average degree of the network. Identifies nodes which mediate many of the short path lengths between other nodes
n-to-1 connectivity	Calculated as the sum of the connectivity degrees between a given node with all other nodes in the network. Measures the amount of information that the given node receives from the rest of the network
Outdegree	A directed graph measure; calculated as the number of edges pointing out of a given node, reflecting the number of outgoing connections. High outdegree identifies nodes that act as sources of information flow
Small world index	Calculated as the normalized ratio of the clustering coefficient to the characteristic path length. Networks with small-world architecture have small-world index >1, along with clustering coefficient >1 and characteristic path length ≈ 1
Strength (mean absolute correlation)	Calculated as the average of the absolute value of the correlations between a node and all other nodes

- **Graph theoretical findings in the healthy brain connectome?**
  - Graph theoretical analyses have consistently demonstrated a small-world topology, an architecture characterized by high path –length and clustering.
  - Structural and functional connectomes have been shown to be composed out of different subnetworks associated with several highly interconnected hub regions mediating the connectivity between different modules.
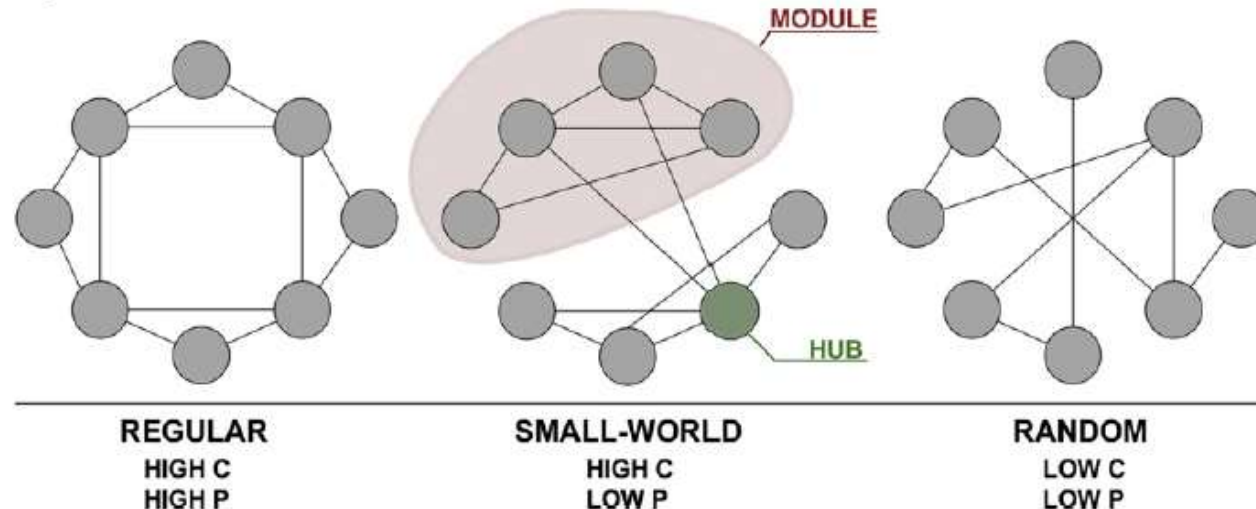

The interplay between clustering and path length can categorize network topology. Regular lattice networks have high clustering and path length; random networks, on the other hand, have low clustering and path length. Small-world networks have high clustering and low path length and, thus, combine a locally and globally efficient organization. Modules (groups of densely interconnected nodes) and hubs (nodes with a high relevance for network connectivity) are frequently observed in small-world networks

Boris C. Bernhardt et al. Epilepsy & Behavior 50 (2015) 162–170

- **JB Kim et al. (Epilepsia, 2014; 55:592–600)**
  - thalamic seed-based functional connectivity (FC) analysis in patients with IGE(N=49) vs. Control(N=42)
    - 1st step: VBM to detect abnormal thalamic region
    - 2nd step: Thalamocortical FC analysis using rfMRI
    - 3rd step: correlation with frontal cognitive performance and clinical variable
  - **Results:**
    - Neuropsychological assessment: ↓performance in patients with IGE than controls
    - VBM: ↓ GM volume in the anteromedial thalamus in patients relative to controls.
    - FC analysis (seed=AMT): ↓ thalamocortical FC in the **bilateral medial prefrontal cortex** and **precuneus/posterior cingulate cortex**
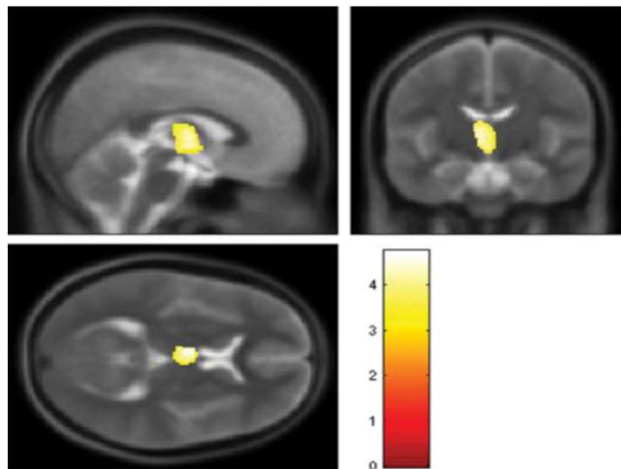
Statistical parametric maps (SPMs) showing a significant gray matter volume reduction in the anteromedial thalamus in patients with idiopathic generalized epilepsy compared to controls
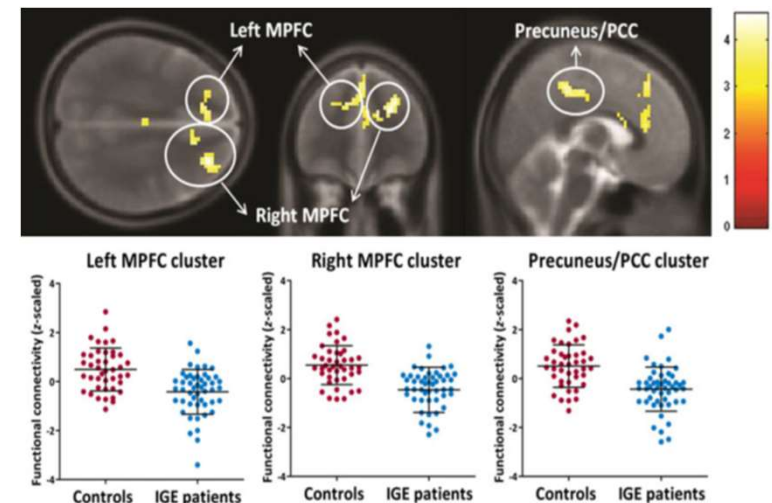
Group differences in resting-state functional connectivity (FC) between patients and controls.

- **J O'Muircheartaigh,et al.,** (Brain 2012: 135; 3635–3644)
    - N= 28 patients with JME (vs. 28 healthy controls)
    - DTI and task-fMRI (phonemic verbal generation)
    - ↓ connectivity from Thalamus(anterior and ventral thalamus) to the prefrontal cortex and SMA
    - Altered task-modulated FC in the frontal cortex directly connected to the thalamus via the same TC-network

Figure 1 Thalamo–cortical bundles showing reduced tractography-defined connectivity between normal subjects and patients with juvenile myoclonic epilepsy (blue, P50.05, corrected for multiple comparisons; red, P50.05, uncorrected) relative to healthy controls. Images on the right show the regions in the thalamus from which the bundles originate.
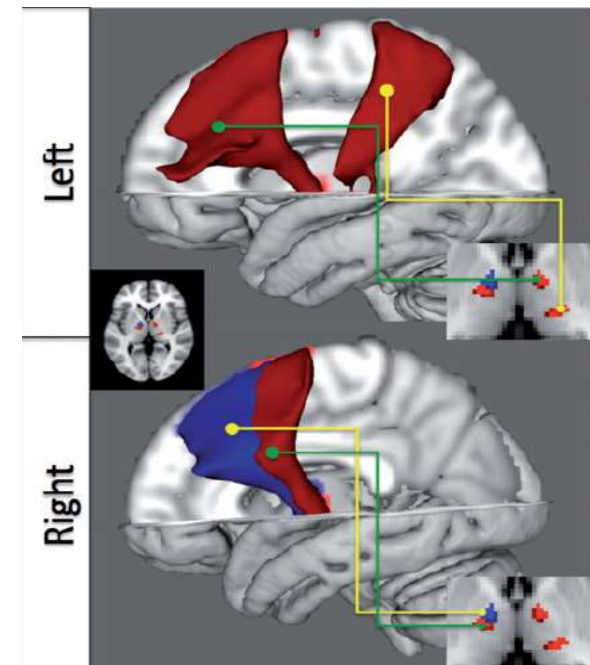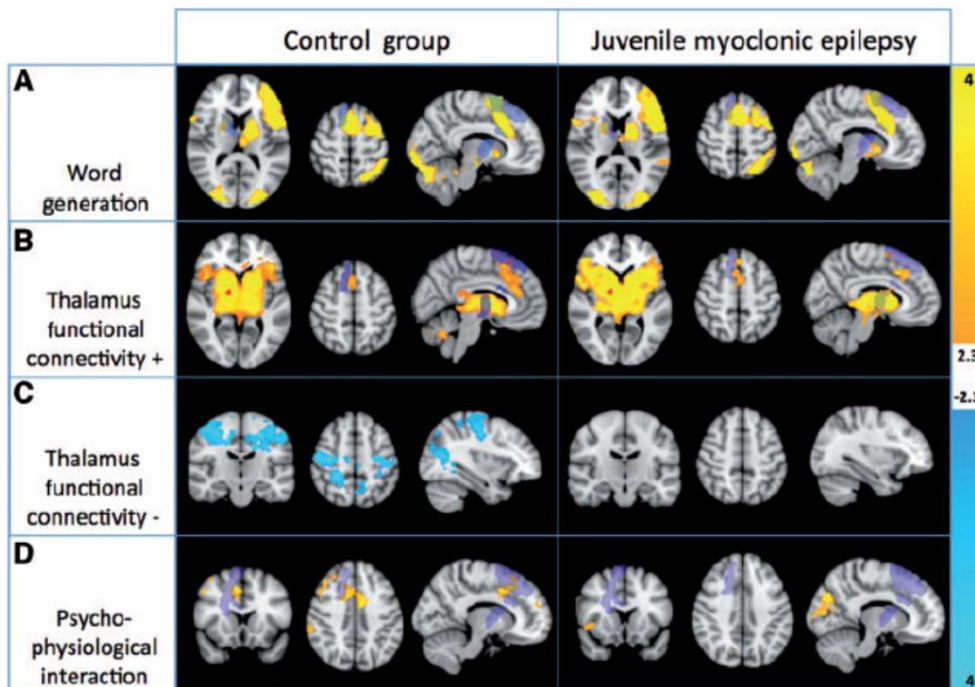

Figure 2 Group average results for each group for the word generation task (A), positive (B) and negative (C) correlation with the thalamic seed region, and psychophysiological interaction between the thalamic seed time series and the task (D). This interaction is negative, indicating a relative failure of this thalamic region to reduce premotor activity .i.e. functional connectivity decreases as a function of task performance. The thalamic bundle defined by the DTI analysis is overlaid in purple.

- **Graph theoretical finding in patients with TLE?**
  - Several graph theoretical analyses on connectomes derived from different modalities have shown topology-level alterations
- **van Diessen et al.** (PLoS ONE 2014; 9(12): e114606)
  - A meta-analysis of 12 studies focused at the average path length and clustering coefficients
  - Compared to control group, Epilepsy group showed
    - ↑ average path length of 0.29 (95% confidence interval (CI): 0.12 to 0.45, p50.0007)
      - → suggests a less integrated global network.
    - ↑ standardized mean average clustering coefficient of 0.35 (CI: 0.05 to 0.65, p50.02)
   - → a more segregated local network.
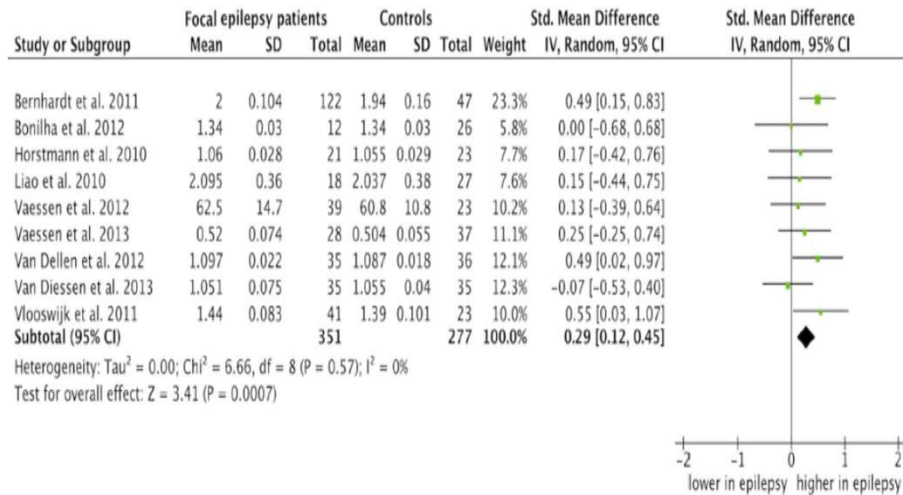
Meta-analysis of the average path length.
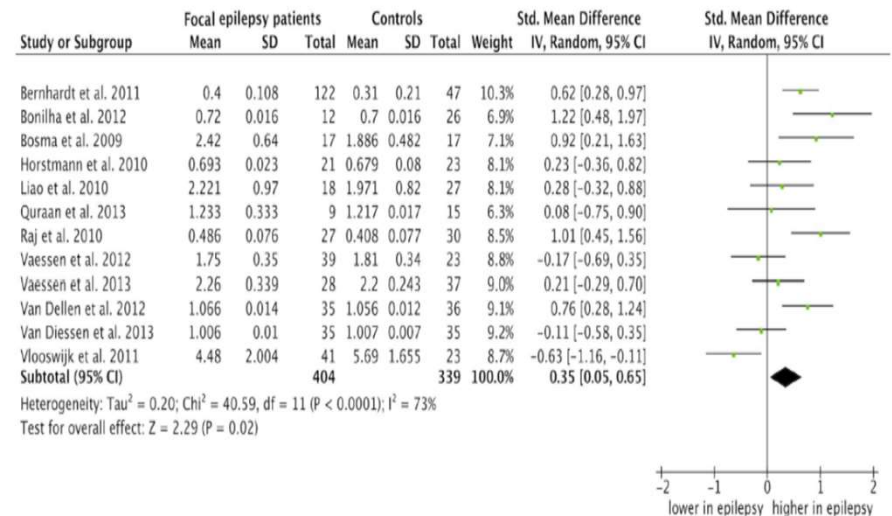
Meta-analysis of the average clustering coefficient.

- **SS Keller et al.** (ANN NEUROL 2015;77:760–774)
  - 87 patients with mTLE (Postop SZ Free in 47 and Not- SZ free in 40) and 80 HC
    (All patients had unilateral HS)
  - Series of Studies
    - Structural MRI: (1) preoperative volumetric analysis of the hippocampus and entorhinal cortex;
      (2) preoperative voxel-based morphometry (VBM) for analysis of whole brain atrophy;
      (3) delineation of surgical lacunae on postoperative MRIs.
    - DTI: abnormal region of brain detected by VBM
  - RESULTS
    - Volumetry of Hipp and EC: no differences between SF vs. not-SF
    - VBM: More widespread and significant atrophy of thalamus in both hemispheres in not-SF than SF
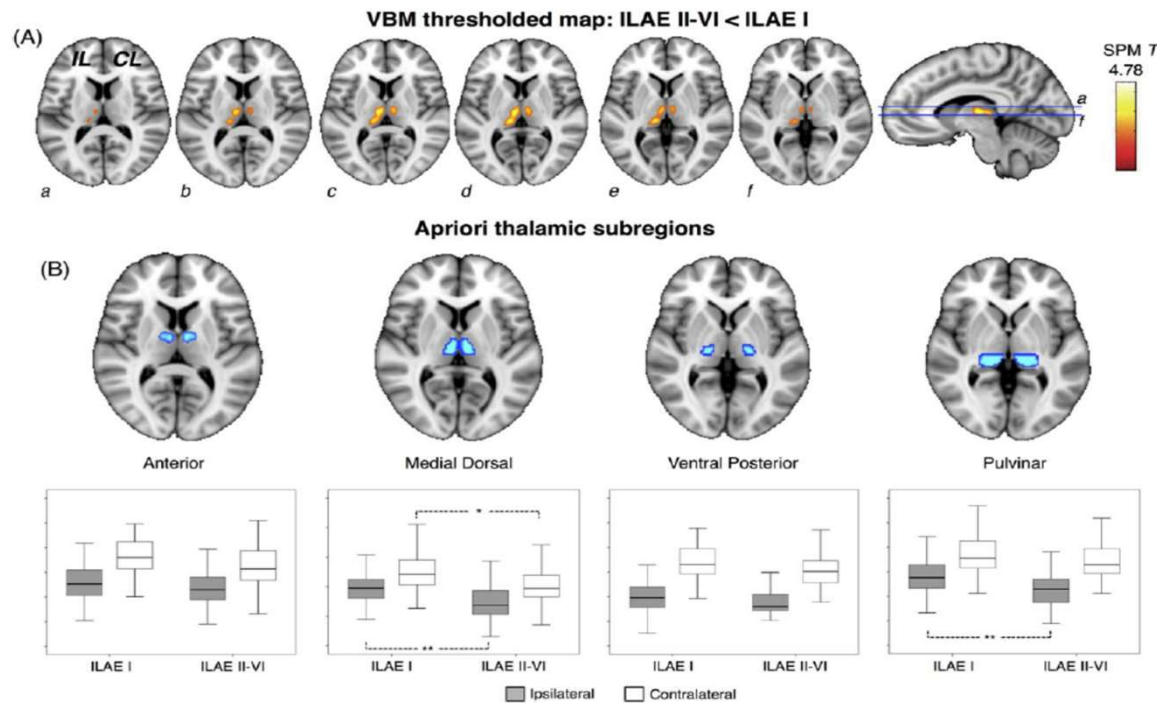

ipsilateral medial dorsal and pulvinar, and contralateral medial dorsal regions were significantly atrophic in patients with persistent postoperative seizures relative to those rendered seizure free.

- **K M Park et al.,**(Journal of Neurology 2020; 267:1179–1187)
- The study was performed independently at two Hospital cohorts (Group A; n=38 and B: n=46).
  - All were newly diagnosed with FU ≥ 6 mo, No MRI lesion
  - Good responders(N=64, seizure free ≥ 6 months) vs. Poor responders(N=20)
  - DTI and Graph theoretical analysis
- The **assortative coefficient** was significantly higher in the AED good responders in both Groups A (0.0239 vs. − 0.0473, p = 0.0110) and Group B (0.0173 vs. − 0.0180, p = 0.0024).
- The time to failure to retain the first AED: significantly longer in patients with assortative networks (n=39:46%) than the disassortative group(n=45: 54%)
- **Conclusion:** We suggests that the brain connectivity could be a biomarker for predicting the responses to AED.
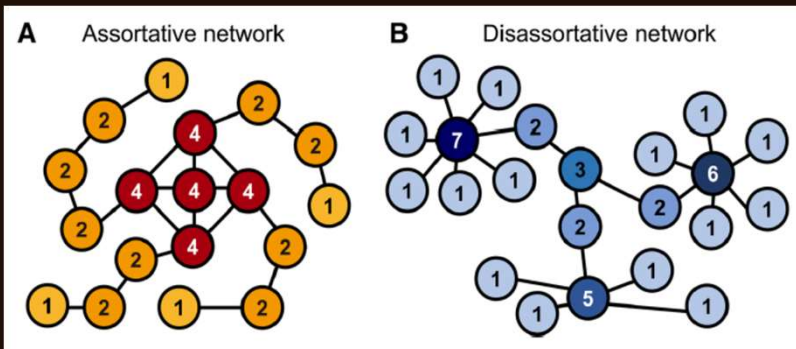
An illustration of assortative and disassortative networks. The assortative coefficient is a measure of the tendency of nodes being connected with similar properties. Networks are called assortative if the nodes connect preferentially with nodes of similar degree, whereas they are called disassortative if the nodes connect preferentially with nodes of different degree. Assortative networks are more robust against removal of their highest degree vertex, while disassortative networks percolate are more vulnerable to attack
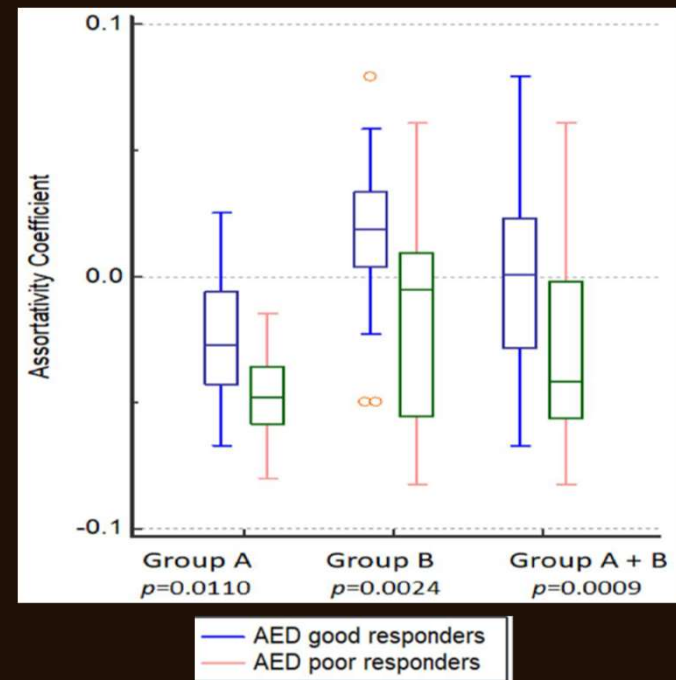
- **Alteration of Functional Connectivity in Response to Treatment in Infantile Spasm**
- **DW Shrey et al**. (Clinical Neurophysiology 129 (2018) 2137–2148)
  - EEG functional connectivity before and after treatment in 21 patients with Epileptic Spasm (vs. 21 HC)
  - Pretreatment EEG: Stronger, more stable functional networks than controls.
  - Posttreatment EEG: FC strength was decreased in all responders (defined by cessation of spasms), but not in non-responders.
- **Conclusions:** Changes in network connectivity and stability correlate to treatment response for ES, and high pre-treatment connectivity may predict favorable short-term treatment response. Functional networks may be an objective markers of treatment response in IS
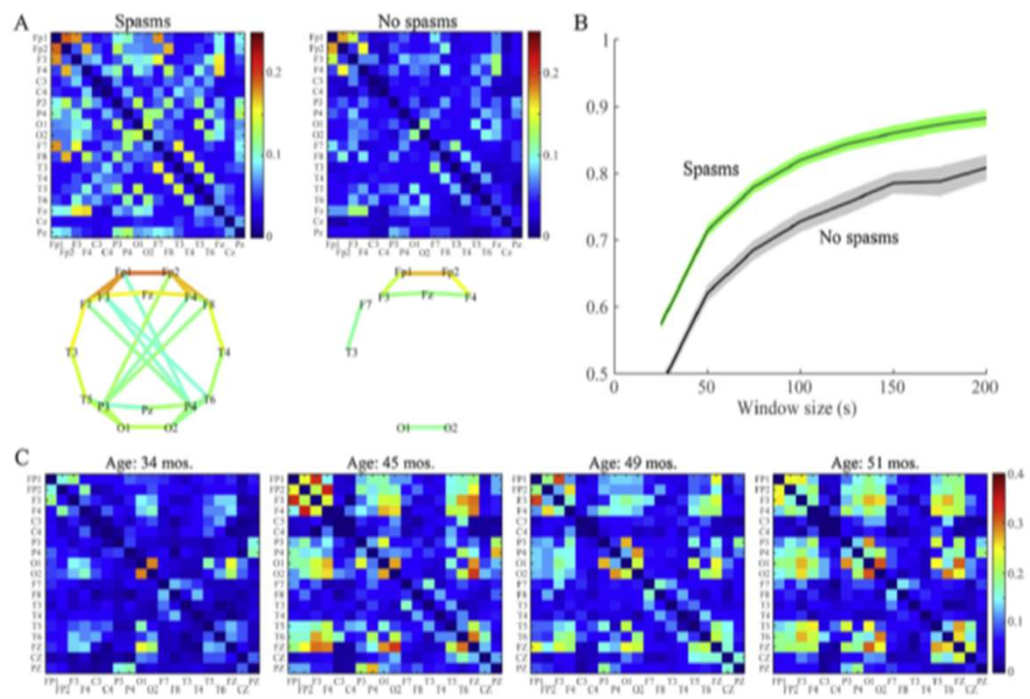

Fig. 6. Epileptic spasms are associated with strong, stable functional networks. (A) Average functional connectivity matrices (top row) and network maps (bottom row) for patients with and without spasms. Network maps show all connections with strength>0.1. (B) Test-retest reliability of the FCN for the spasms group (green) and the non-spasms group (gray) measured via 2D correlation of the connectivity matrices for EEG segments of varying length. FCNs are reliable when measured using segments of EEG at least 150 s long, and the spasms group exhibited higher reliability than controls. (C) A representative example of FCNs from longitudinal EEGs of a patient who had spasms and was diagnosed with Lennox-Gastaut at 45 months old. The strength of the FCN increases with onset of Lennox-Gastaut and varies over time; however, note that the locations of the strongest connections in the network remain stable over the 17 month period. This patient experienced continued seizures, despite multiple medication changes.
From Stacey et al. (Epilepsy Research 159 (2020) 106255)

- **GM Ibrahim et al.** (NeuroImage: Clinical 16 (2017) 634–642)
  - Hypothesis: unique pattern of TC connectivity are assoicated with SZ response following VNS
  - Discovery cohort (N=21): Responsders=11 vs. Non-responders=10
    External cohort (N=8)
- **Method:** rfMRI before and after VNS implantation and manual drawing of thalamic ROI
    Mean time series correlations of the ROIs with all voxels in the brain
    Development of Support Vector Machine(SVM) learning algrithm (by supplying known sets of inputs and responses to the data)
    Sensitivity and specificity of the SVM Model was plotted in the ROC curve
- **Results:** ↑ connectivity between the Lt Thalamus and anterior cingulate/ventromedial prefrontal cortex(ACC/vmPFC) and bilateral operculoinsular cortex in responders
    ↑ connectivity between Rt Thlamus and ACC/vmPFC and Lt insular cortex
- The SVM model correctly classified response to VNS with 86% accuracy and, in an external cohort of 8 children, correctly classified with 88% accuracy
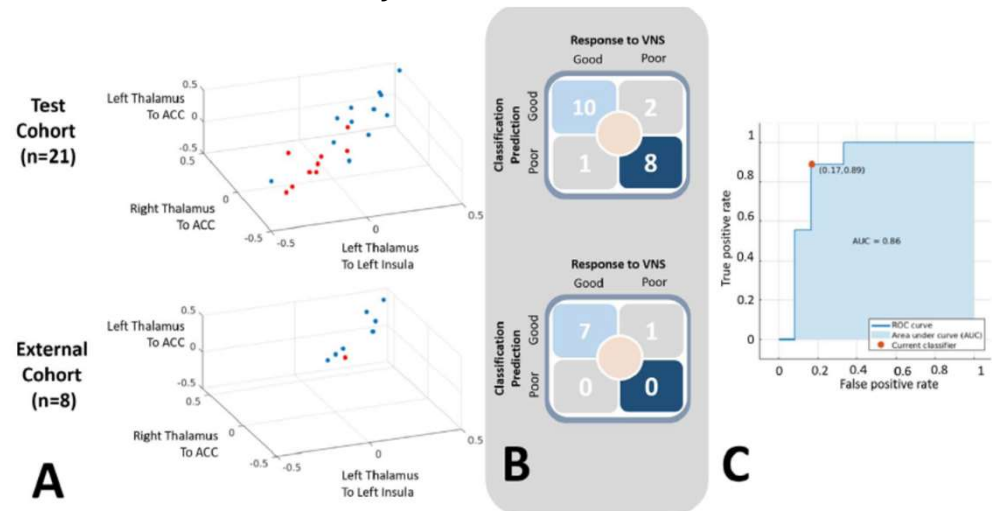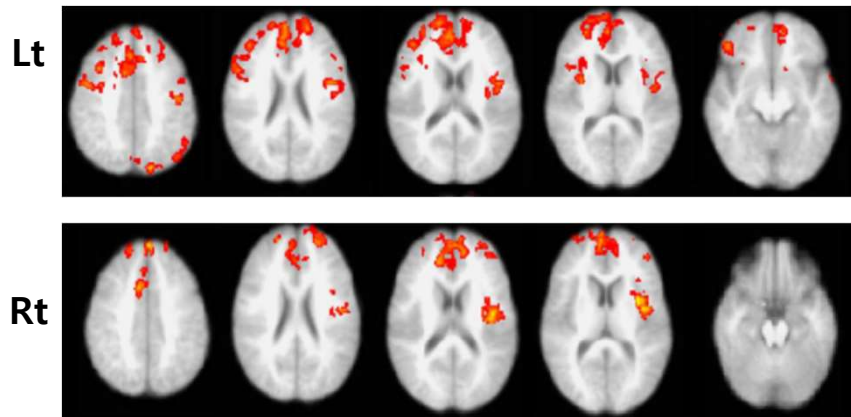
Generalized linear model of the left and the right thalamic whole-brain connectivity regressed against selected covariates. In children with good seizure response to VNS,

(A) Classification of response to VNS on the basis of TC connectivity: Blue → good, red → poor response to VNS. (B) On the basis of TC- connectivity to the ACC/Lt insular cortex, linear SVM classified with an 86% accuracy in the test cohort (n =21) and 88% in the external cohort (n = 8). (C) The ROC curve to identify VNS responders

- **Karim Mithani et al.** (ANN NEUROL 2019;86:743–753)
  - Discovery cohort(N=28) and Validation cohort(N=18)
  - DTI to identify group differences in white matter microstructure, which were informed to the beamforming of MEG Support Vector Machine learning classifier
- Results:
  - ↑FA in the Lt TC, Limbic, and association fibers with ↑FC in the networks involving Lt Thalamic, insular and temporal nodes
  - SVM classifier demonstrated 89.5% accuracy and area under the ROC curve of 0.93. In the external validation cohort, this model demonstrated an accuracy of 83.3%, with a sensitivity of 85.7% and specificity of 75.0%.
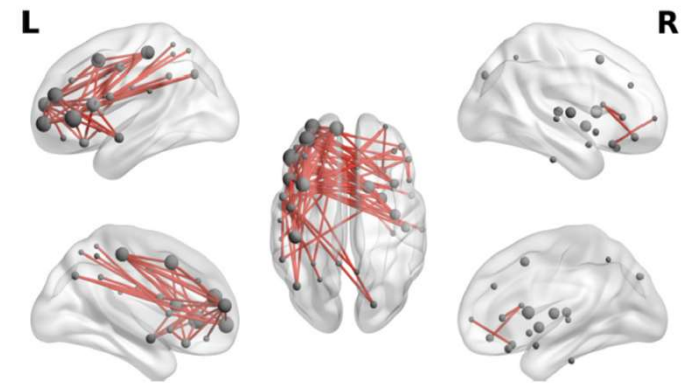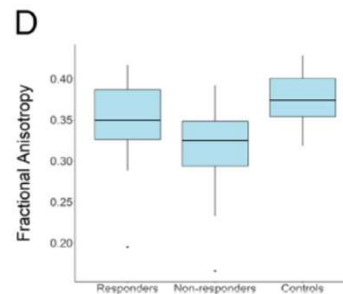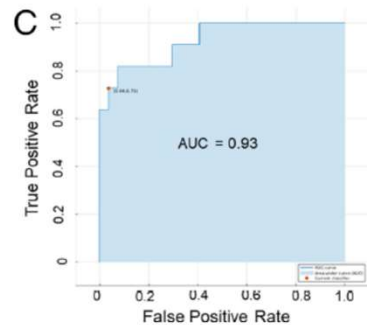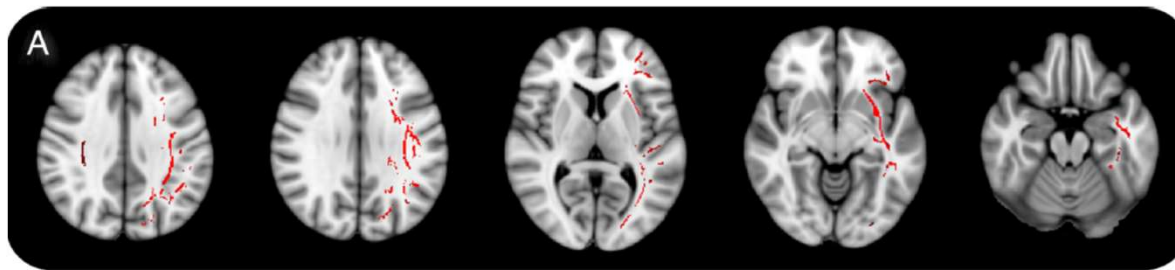
(A)Whitematter tracts with greater FA in VNS- responders compared to nonresponders. These encompass thalamocortical, limbic, and association fibers. (B) Confusion matrix of SVM classifier based on DTI-data. (C) ROC curve of the SVM classifier, showing high accuracy on 10-fold cross-validation. (D) Average fractional anisotropy of the significant white matter tracts,, showing that responders' circuitry is more similar to controls than nonresponders.

MEG-analysis, showing a significantly stronger functional network expression in responders relative to nonresponders encompassing insular, thalamic, and cortical nodes. Results are shown for alpha frequency (7.5–12Hz).

III. Recent Progress and Future Perspectives

- Epilepsy is a Network Disease → Network Analysis may be a fundamental tool to understand the neurobiology of epilepsy

- Rapid progress in Diagnostic technologies and Computer science → Expansion in the size, scope and complexity of neural data, « Big Data »,

- Development of innovative Models with Machine Learning techniques are more widely applied to test the organization of a Network's connections at global and local scales, which are essential for the identification of primary epilepsy network and therapeutic interventions

- We are entering into the Era of Network Neuroscience, a new frontier of Neuroscience, which requires a Network of Neurologists, Physicist, Mathmaticians, and Computer scientists, etc.

Thanks for Your Attention